Developmental Biology 448 (2019) 320–341

Contents lists available at ScienceDirect

Developmental Biology

journal homepage: www.elsevier.com/locate/developmentalbiology

IAP genes partake weighty roles in the astogeny and whole body regeneration in the colonial urochordate *Botryllus schlosseri*

Amalia Rosner[a,*], Olha Kravchenko[a,b], Baruch Rinkevich[a]

[a] Israel Oceanographic & Limnological Research Institute, Tel Shikmona, P.O.B. 8030, Haifa 31080, Israel
[b] National University of Life and Environmental Sciences of Ukraine, Heroiv Oborony, Str 17, building 2, of 45, Kyiv 03041, Ukraine

ARTICLE INFO

Keywords:
Apoptosis
Brinapant
Blastogenesis
Botryllus schlosseri
Budectomy
GDC-0152
IAP
Regeneration
Smac mimetics
Wnt agonist
Zooidectomy

ABSTRACT

Inhibitors of Apoptosis Protein (IAP) genes participate in processes like apoptosis, proliferation, innate immunity, inflammation, cell motility, differentiation and in malignancies. Here we reveal 25 IAP genes in the tunicate *Botryllus schlosseri's* genome and their functions in two developmental biology phenomena, a new mode of whole body regeneration (WBR) induced by budectomy, and blastogenesis, the four-staged cycles of botryllid ascidian astogeny. IAP genes that were specifically upregulated during these developmental phenomena were identified, and protein expression patterns of one of these genes, IAP28, were followed. Most of the IAP genes upregulation recorded at blastogenetic stages C/D was in concert with the upregulation at 100 μM H_2O_2 apoptotic-induced treatment and in parallel to expressions of AIF1, Bax, Mcl1, caspase 2 and two orthologues of caspase 7. Wnt agonist altered the takeover duration along with reduced IAP expressions, and displacement of IAP28$^+$ phagocytes. WBR was initiated solely at blastogenetic stage D, where zooidal absorption was attenuated and regeneration centers were formed either from remains of partially absorbed zooids or from deformed ampullae. Subsequently, bud-bearing zooids developed, in concert with a massive IAP28-dependent phagocytic wave that eliminated the old zooids, then proceeded with the establishment of morphologically normal-looking colonies. IAP4, IAP14 and IAP28 were also involved in WBR, in conjunction with the expression of the pro-survival PI3K-Akt pathway. IAPs function deregulation by Smac mimetics resulted in severe morphological damages, attenuation in bud growth and differentiation, and in destabilization of colonial coordination. Longtime knockdown of IAP functions prior to the budectomy, resulted in colonial death.

1. Introduction

Botryllus schlosseri (Urochordata, Ascidiacea), taxonomically classified within the closest relatives of the vertebrates, is a perfect model species for studying complex biological mechanisms like apoptosis, aging, allorecognition, regeneration and more (Ballarin et al., 2008; Manni et al., 2007; Rinkevich, 2002). *B. schlosseri* is a hermaphrodite colonial ascidian, composed of up to thousands of genetically identical modules (each called a zooid). Three successive generations of modules contemporaneously reside in adult colonies at any given time throughout the colony's lifespan; the mature filtering zooids and two cohorts of buds, the differentiating primary buds that are connected to the zooids, and secondary buds (budlets), emerging from the primary buds. The differentiation and the lifespan of the modules within a colony are genetically controlled and synchronized, so that modules of a certain generation are all exactly at the same differentiating status (Manni et al., 2014).

Astogeny is manifested by weekly repeating blastogenesis cycles (in colonies grown at 20 °C). The blastogenetic cycle is divided into discrete stages following two staging practices. One introduced by Berrill (1951) and revised recently by Manni et al. (2014) divides the blastogenetic cycle into 11 stages based on the budlets, primary buds and zooids integrated developmental stages. The second staging method, used in this work, divides the blastogenetic cycle into 4 major stages (A-D; Fig. 2a-d; sensu Mukai and Watanabe, 1976a). Stage A starts with the opening of the zooidal oral and excurrent siphons. Stage B initiates with the beginning of heartbeats in the primary buds, while stage C begins with onset of organogenesis in secondary buds and the accumulation of pigment cells in the epithelium of the primary buds. The last stage D commences with the shutdown of oral and excurrent siphons. In stage D (last 24–36 h), all mature zooids die in a stepwise, anterior-to-posterior, synchronized wave of massive apoptosis and phagocytosis processes (the takeover stage; Ballarin et al., 2010; Cima et al., 2010; Lauzon et al., 1993). Meanwhile, the primary buds are transformed to functional zooids, the budlets turn into primary buds and a new generation of budlets (up to 4 per zooid) is formed (Manni et al., 2014). Reproductive processes, such as oogen-

* Corresponding author.
E-mail address: amalia@ocean.org.il (A. Rosner).

https://doi.org/10.1016/j.ydbio.2018.10.015
Received 14 June 2018; Received in revised form 29 September 2018; Accepted 17 October 2018
Available online 30 October 2018
0012-1606/

esis, spermatogenesis and embryogenesis, are synchronized with the blastogenesis, so that ovulated eggs are ready the moment a new generation of zooids emerges, and then are fertilized by sperm arriving from other colonies at advanced stages of blastogenesis. The newly formed larvae swim out of the zooids just prior to the onset of the takeover phase (Berrill, 1950, 1951; Milkman, 1967; Mukai and Watanabe, 1976a, 1976b).

In *B. schlosseri,* a vascular budding process (a form of whole body regeneration; WBR) is experimentally induced by removing all zooids and buds from the colony (Sabbadin et al., 1975; Voskoboynik et al., 2007). In contrast to the congener *Botrylloides leachi* WBR (Rinkevich et al., 2007), *B. schlosseri* WBR is induced only during the takeover phase, and the first set of zooids are still smaller than normal modules.

Inhibitors of Apoptosis (IAPs), a family of proteins first identified as regulators of caspases and cell death, were later revealed as multi-functional, participating in proliferation, cell cycle, signaling, cell motility, inflammation, innate immunity and cancer (Budhidarmo and Day, 2015; Estornes and Bertrand, 2015; Fulda, 2014a, 2014b; Silke and Meier, 2013; Vasilikos et al., 2017; Vasudevan and Ryoo, 2015). IAP genes exist in a variety of organisms, from viruses to mammals, but their exact numbers differ (yeast-one; *Drosophila*-four; humans-eight). IAPs are characterized by one to three 70aa zinc-binding BIR (baculovirus IAP repeat) domains that modulate protein-protein interactions and are required for the anti-apoptotic activity of IAPs. There are two types of BIR domains (type I and II), classified according to the presence (type II) or absence (type I) of a 'deep' peptide-binding structural groove (Gyrd-Hansen and Meier, 2010). Type II BIR domains interact with proteins having a domain called IBM (IAP-binding domain) that exists in activated caspases or in IAP antagonists like SMAC (Second Mitochondrial Activator of Caspases). Type I BIR interacts with proteins like tumor necrosis factor receptor (TNFR) associated factor 1 and 2 (TRAF1 and TRAF2). In addition to the BIR domains, IAP proteins may contain conserved domains at the C terminal of the molecule. Most frequent is the RING (Really Interesting New Gene) domain that functions as an E3 ubiquitin ligase acting in the ubiquitin-proteasome pathway, promoting auto-ubiquitination, cross-ubiquitination of other IAPs or other substrates (Ma et al., 2006). A UBA (ubiquitin associated) domain may appear together with a RING domain and function in binding single or chains of ubiquitin repeats existing on other proteins, thus enabling complex assembly and signal transductions (Blankenship et al., 2009). Additionally, UBC (Ubiquitin-conjugating) domain (Martin, 2004) is typically expressed in BIRC6 (Apollon). IAPs are the only endogenous proteins capable of suppressing both initiator and effector caspases (O'Riordan et al., 2008) and are known in regulating the NF-κB signal transduction pathway (Gyrd-Hansen and Meier, 2010), and in the absence of IAPs, in some organisms like *Drosophila*, initiator caspase is activated and apoptosis is induced (Silke and Meier, 2013). IAP expressions vary in different tissues, between embryos and adults, between physiological states and between healthy to transformed tissues (Altieri, 2015; Dallaglio et al., 2012; De Maria and Bassnett, 2015).

Here we revealed the IAP gene family in *B. schlosseri* (25 genes, 9–11 subfamilies based on IAPs domains). Gene functions were studied along with the blastogenetic cycle and during budectomy induced WBR. We identified IAP genes that are specifically upregulated during these processes, and five of the upregulated IAPs in blastogenetic stage D colonies, that are further upregulated in blastogenetic stage A colonies exposed to 100 μM H_2O_2. The protein expression patterns of one of these genes, IAP28, in various tissue and blastogenetic stages, are described in detail. Block of IAP genes functions resulted in morphological changes and upregulation of caspase 9 mRNA in treated blastogenetic stage A colonies. In budctomy-induced WBR, IAP malfunction curtailed the regeneration and induced complete death of the tissue. IAP28, Pl10, Vasa and phospho-Histone H3 expression patterns were further studied to understand the ongoing mechanisms in a colony following budectomy. Finally, we describe possible interactions between IAP gene expressions, regeneration and the Wnt, as the pro-survival Akt/GSK-3beta pathway.

2. Materials and methods

2.1. Animals

B. schlosseri colonies collected at Monterey, Half Moon Bay and Moss Landing Marinas in California, were shipped to the seawater facility at the National Institute of Oceanography (Haifa, Israel) and were reared at 20 °C as described by Rinkevich and Shapira (1998).

2.2. Subcloning

Large *B. schlosseri* colonies were cut between systems into colonial fragments (ramets), each containing 2–3 systems. Each ramet was detached from the glass slide substrate using a razor blade and placed on a new glass slide. Excess water was dried and the slides were place in a humid chamber for 30 min. Thereafter, the slides were carefully placed into seawater tanks and allowed to acclimate for at least two weeks.

2.3. Budectomy induced whole body regeneration

Budectomy is the excision of all the buds from a colony. *B. schlosseri* colonies were incised into two parts by cutting out a tissue segment of 0.5–1 cm width from the middle of each colony, leaving the two remaining parts on the same glass. One part of each colony was then budectomized while the second remained intact and served as control. The budectomy was performed on ramets in various blastogenetic stages, while the phenotypic change in the colony was identified only after the onset of takeover. The colonies were observed daily and analyzed for morphological changes one month following budectomy.

2.4. RNA extraction and cDNA synthesis

Total RNA was extracted using RNeasy Mini Kit (cat. no 74106; QIAGEN, Hilden, Germany) following manufacturer instructions. DNA was removed using RNase-Free DNase Set (cat. no 79254; QIAGEN, Hilden, Germany). The DNase enables on-column digestion of DNA during RNA purification using the RNeasy kit.

cDNA synthesis was performed with RevertAid First Strand cDNA Synthesis Kit (cat. no K1622; Thermo Fisher Scientific, MA, USA). 2 μg of total RNA per sample was used for cDNA synthesis with random hexamers.

2.5. 3′ RACE reactions

Region 3′ of the IAP gene fragments mined from the *B. schlosseri* database at Stanford were obtained by using the forward appropriate primers whose sequences for each gene are detailed in the file "qPCR primers" (Supplementary material). The SMART RACE cDNA Amplification Kit (Clontech, CA, USA) was used according to the manufacturer's instructions.

2.6. Quantitative PCR and statistical analysis

qPCR amplifications were performed with Fast SYBR™ Green Master Mix (cat.no 4385614; Thermo Fisher Scientific, MA, USA) according to manufacturer instructions using a StepOnePlus Real-Time PCR System (Thermo Fisher Scientific, MA, USA). The relative quantification method $\Delta\Delta C_T$, which was described by Pfaffl (2001) was used to calculate fold change in genes' expressions. 18S rRNA (accession no: AB211066) served as the reference gene. The data was presented as fold change on $\log_2$ scale. Primers used in this analysis are detailed in the file "qPCR primers" (Supplementary material).

The statistical analysis was performed on ΔC_T values of each experiment. Since all experiments assessed changes in ramets originating from the same colony (same genet), differences between the groups following several biological repeats (different genets) were calculated using paired student's *t*-tests or repeated measures ANOVA. A statistical significant difference was considered as $p < 0.05$ using the SPSS 22 software package.

2.7. Chemicals

Smac mimetic and IAP antagonist drugs, GDC-0152 and Birinapant, are generally used for the treatment of solid tumors and hematologic cancers.

We adopted Birinapant's (TL32711; ApexBio Technology, cat. no A4219) recommended dosage from Perimenis et al. (2016). Accordingly, we submersed *B. schlosseri* colonies in seawater containing Birinapant at concentrations of 1.45 mg/l (blastogenesis) or 1.1 mg/l (whole body regeneration).

Dosages of 12.5–100 ng/ml (Hu et al., 2015) of GDC-0152 (ApexBio Technology, cat. no A4224) are known working concentrations on cell lines. We calibrated the GDC-0152 working concentrations following repeated incubations establishing 2 mg/l GDC-0152 for studying impacts on the blastogenetic cycle and 1 mg/l for studying impacts on regeneration following budectomy.

Hydrogen peroxide (H_2O_2; Sigma-Aldrich, cat. no 31642) was used at concentrations of 100 μM and 1000 μM.

Wnt agonist (WA) 2-Amino-4-(3,4-(methylenedioxy)benzylamino)-6-(3-methoxyphenyl)pyrimidine hydrochloride, (Sigma-Aldrich, cat. no. SML0698) was used at a working concentration of 0.05 μM.

2.8. Western Blot

Total proteins were extracted as described by Rosner et al. (2013). 14 μg of protein was loaded per lane. The Western blotting analysis was adapted for Odyssey detection kit and performed as recommended by the manufacture (http://biosupport.licor.com/docs/Western_Blot_Analysis_11488.pdf), with Anti-Rabbit IgG (IRDye 800CW 611-131-002S., Rockland, PA, USA) as a secondary antibody.

2.9. Antibodies and immunohistochemical analyses

2.9.1. Primary antibodies

Rabbit anti *B. schlosseri* IAP28 polyclonals were elicited against the sequence GDNPEDRRWHKPTC. The polypeptide was coupled to chicken albumin and used to immunize two rabbits (Hy-labs Biotechnologies, Rehovot, Israel). Working concentration was 1:2000.

Polyclonals anti-Pl10 and polyclonals anti-Vasa antibodies were elicited in rabbits; working concentration 1:4000 (Rosner et al., 2006, 2009, respectively).

Anti-phospho-Histone H3 (pH3) rabbit polyclonals (Ser 10)-R: sc-8656-R Santa Cruz; working concentration 1:400.

2.9.2. Secondary antibodies

Cy™3-conjugated AffiniPure Goat anti-rabbit IgG (H+L) Amax-550; Emax 570. Cat. No. 111-165-003 (Jackson ImmunoResearch laboratories, Inc.).

Cy™5-conjugated AffiniPure goat anti-rabbit IgG (H+L)Amax: 650 Emax: 670 nm Cat No. 111-175-144 (Jackson ImmunoResearch laboratories, Inc.).

The immunohistochemical analyses were performed as described in Rosner et al. (2013), with the following modification: the solution used for heat-induced epitope retrieval was Tris-EDTA buffer (10 mM Tris Base, 1 mM EDTA Solution, 0.05% Tween 20, pH 9.0). The stained sections were observed under a Nikon eclipse Ni Microscope.

3. Results

3.1. The IAP gene family

The *B. schlosseri* genomic library (Voskoboynik et al., 2013) was searched for IAP genes. A serial number was assigned to each identified gene (or gene fragment) for ease of handling, and the matching key for the gene numbers in the database is available in the file 'qPCR primers' (Supplementary material). The sequences of these genes (partial or complete) are accessible in the file 'IAP sequences' (Supplementary material). The IAP sequences were compared to each other using the online multiple sequence alignment package 'T-Coffee' (https://www.ebi.ac.uk/Tools/msa/tcoffee/) to avoid redundancy. Twenty-five unique sequences (Fig. 1), each containing at least one BIR domain, were further compared to two additional *B. Schlosseri* transcriptome databases available online (Campagna et al., 2016, http://botryllus.cribi.unipd.it; De Tomaso et al., 2012, http://octopus.obs-vlfr.fr/public/botryllus/blast_botryllus.php) as quality control and a precaution step. We amplified and sequenced the 3′ ends of these genes by the 3′ RACE method. Determining the 3′ sequence of the genes serves two purposes: (1) to classify the IAP proteins at the C terminus, where additional domains besides the BIR exist; (2) as an additional tool to detect redundancy. This was accomplished for 18 out of the 25 genes studied. The RING domain was detected in 16 out of the 18 genes, and in 7 genes, the UBA domain was located 5′ to the RING domain. IAP21, the homologue of human Apollon (Schläfli et al., 2012), carried one BIR and one UBC domain at the 3′, and IAP7 contained just two BIR domains (Fig. 1). The seven genes, that we failed to establish their 3′ terminus, were isolated and sequenced, implying that they indeed are part of the *B. schlosseri* genome. The three genes of group I and the gene of group J, contain three BIR elements (Fig. 1). Since the number of BIR elements per gene is maximum three, and the genes in groups I & J do not have any significant sequence similarity to any of the genes in groups A-H, it was concluded that groups I & J signify different genes than those found in groups A-H. However, we could not exclude the possibility that they might be part of group A or group D. Group K contain three gene fragments which we were not able to classify. Therefore, the number of *B. schlosseri* groups or subfamilies has been defined at this stage as being between 9 and 11.

Blastx alignment of IAP sequences against the NCBI database revealed that 21 out of the 25 genes had the highest sequence identities to IAP genes of the solitary tunicate *Ciona intestinalis* (32–54%). Four genes: IAP 9, 17, 21, 23, showed the highest similarities to IAP genes of other organisms. In each of these IAPs, the identity to its closest homologue was below 30%.

3.2. Expression throughout the blastogenetic cycle

Each of twelve genetically different *B. schlosseri* colonies was subcloned into four ramets (n = 48) that were acclimatized and sacrificed, so that for each genet either one of the four blastogenetic stages was represented (Fig. 2a-d). mRNA expressions of various genes were compared by relative qPCR analyses in each genet separately. At least four different genets (biological repeats) were analyzed for each gene. We analyzed the expressions of 25 IAP genes, 5 caspases (initiator caspases casp2, casp9 and executioner caspases casp3 and two homologues casp7: 7.1 and 7.2), three pro-apoptosis regulating genes (AIF1, Bax and Mcl1), genes regulated by the Wnt pathway (Myc, Sox2, β-Catenin, Cdc25; http://web.stanford.edu/group/nusselab/cgi-bin/wnt/target_genes) known to disrupt blastogenesis (Rosner et al., 2014) and regulate IAP gene expressions. In addition, we analyzed the expressions of genes related to the pro-survival PI3K-Akt Pathway (Akt, PI3Kc, GSK3B; Zhao et al., 2012), Pl10 known to be highly expressed in buds (Rosner et al., 2006) and a modulator of NF-κB transcriptional activity (N. Xiang et al., 2016).

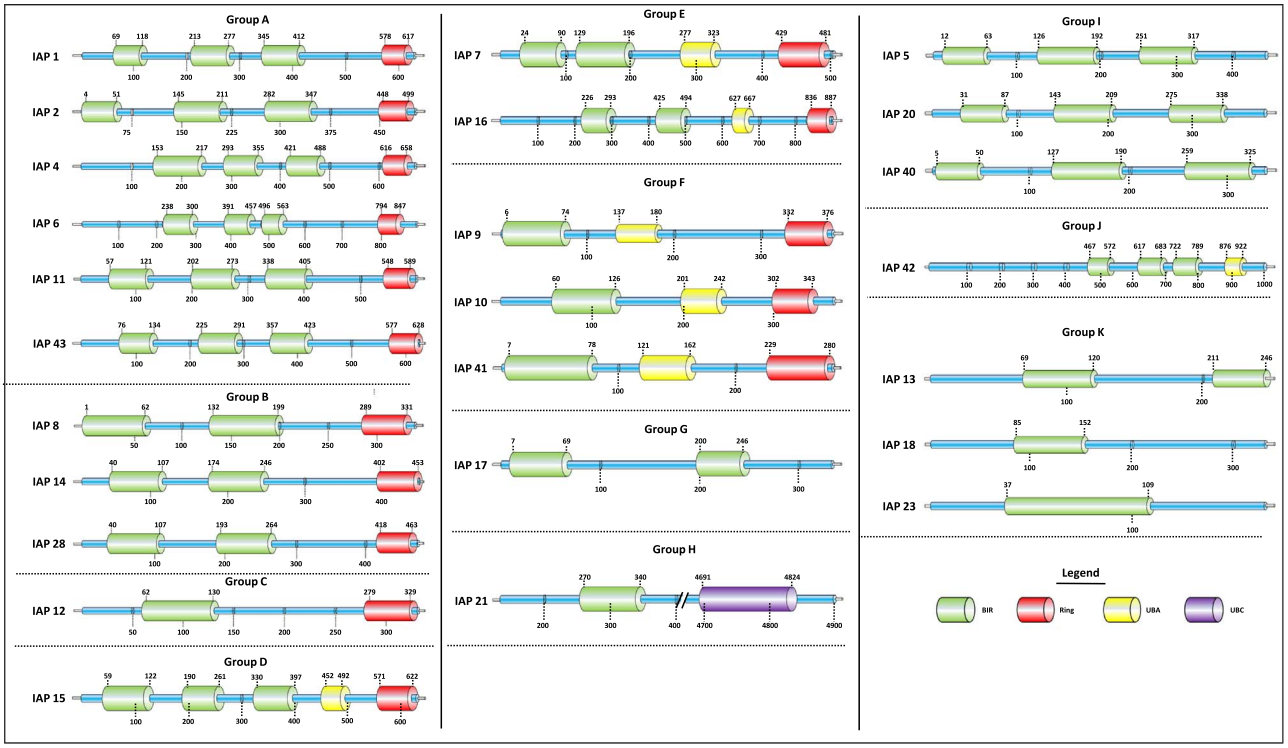

Fig. 1. Schematic illustration of the 25 *B. schlosseri* IAP proteins, their various domains (BIR, Ring, UBA, UBC) and relative positions of the domains on each molecule. The IAPs are divided into 11 subfamilies according to the domains they express.

Fig. 2e shows the average ΔC_T of all IAP genes at each one of the blastogenetic stages. A significant decrease in the average ΔC_T at blastogenetic stages C and D relative to blastogenetic stages A and B implies a surprising increase in average IAP genes expressions towards the second half of the blastogenetic cycle. The average C_T values obtained by qPCR analyses were also used to calculate the fold change in specific gene expression along blastogenesis, relative to blastogenetic stage A (fold changes are expressed as $\log_2$ of the obtained values). Significant differences in gene expression ($p < 0.05$) among the four blastogenetic stages were found using the calculated ΔC_T values and ANOVA repeated measures analysis. Fig. 2f presents the levels of a variety of genes along blastogenetic stages B-D, relative to their expressions at blastogenetic stage A. To simplify the presentation, only genes with statistically significant expression changes among the blastogenetic stages are shown. Table 1 summarizes the P_A values (p-value of ANOVA test) of those genes whose expressions were significantly altered between the various blastogenetic stages, and the p-values represent the post-hoc analyses in the various blastogenetic stages for each gene. Significant upregulated expressions of apoptosis regulators (AIF1, Bax, Mcl1) and caspases (2 and 7.1) were detected at blastogenetic stages C and D. These results are in accordance with the massive apoptotic wave occurring at stage D during zooidal absorption. As described above, the IAP family of genes in general are also upregulated in the takeover stage - primarily IAP8, IAP16, IAP18, IAP21 and IAP28 expressions that are increased by a least 16-fold. IAP8 (contig g7904 in the *B. schlosseri* database) was upregulated at the end of the blastogenetic cycle, in accordance with Campagna et al. (2016). mRNA expressions of the genes related to the pro-survival PI3K-Akt or Wnt pathways were not significantly altered.

The above studies were performed on the whole ramet level, hence, a possible account for the increased mRNA expression of IAP genes at the end of the blastogenetic cycle could be differential built-in quantities in developing buds. Therefore, we surgically isolated zooids, buds and ampullae & tunic and studied the IAP genes expressions of blastogenetic stage A versus stages C & D for each one of these colonial fragments taken from the same colony (X5 biological repeats; Fig. 2g). Results were statistically analyzed using ANOVA repeated measures. We also studied Pl10 and Myc that are known to be upregulated in buds (Rosner et al., 2006; Kawamura et al., 2008), Sox2 and genes of the PI3K-Akt pathway. The results revealed that buds at blastogenetic stages C/D express significantly higher Myc, Pl10 and Sox2 than respective zooids in the same colony. IAP8 and IAP28, both from IAP group B (Fig. 1), exhibited the most surprising expression patterns. They were specifically upregulated (5.9–52 times more) in blastogenetic stage C/D zooids relative to matched buds, the vasculature and to stage A zooids from the same colony. IAP9 was > 47 times upregulated in blastogenetic C/D zooids relative to stage A zooids and 5.7 times upregulated in C/D buds relative to C/D zooids (i.e. about 270 fold increase in stage C/D buds relative to stage A zooids). IAP41 was upregulated in blastogenetic C/D zooids relative to the buds and vascular system (10.73 and 4.56 times, respectively). In contrast, five of the IAP genes (IAP7, IAP15, IAP21, IAP23 and IAP43) were indeed specifically upregulated in stage C/D buds.

IAP8 and IAP28 contain similar domains, i.e. two BIR elements at the N-terminus and a Ring domain at the C-terminus, while not having significant resemblance at the nucleotide level and sharing only 50% identity at the protein level. *B. schlosseri* anti-IAP28 polyclonals were elicited and tested by Western blot analysis performed on stage D zooids whole tissue lysate (Fig. 3a). A band of about 60 kDa was detected, slightly above 53.3 kDa, the calculated molecular weight. For better understanding IAP28 functions, immunohistochemistry analyses with anti-IAP28 polyclonals were performed on various blastogenetic stages (Fig. 3b-j). Analyses in zooids of control *B. schlosseri* colonies revealed high expressions in the stomachs (Fig. 3b), cerebral ganglion (Fig. 3b, c), atrial epithelium and in cells in the connective tissue lining internal organs like the digestive system (Fig. 3f), or the endostyle (Fig. 3g). Few stains were detected in blastogenetic stage B cell islands (CI) in which phagocytes are packed (Fig. 3g), in blood cells and in tunic cells (Fig. 3i). Primary buds at blastogenetic stage A do not express IAP28 (not shown). Buds were first stained in the differentiating neural complex at late blastogenetic stage B and in testes within the gonad sacs (Fig. 3b). Towards the end of blastogenetic stage C and

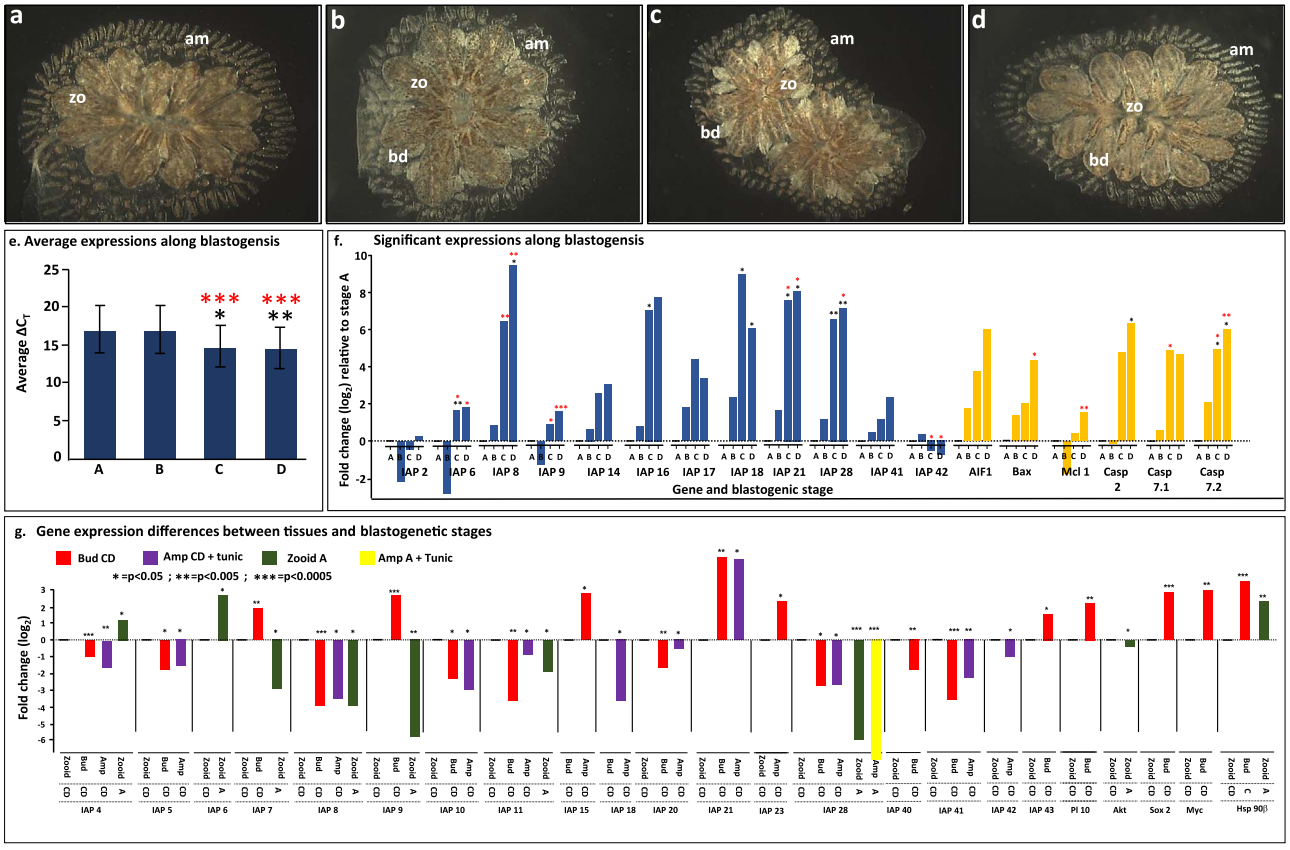

Fig. 2. IAP gene expressions throughout the regular blastogenetic cycle. (a-d) Representative phenotypes of colonies at blastogenetic stages A, B, C and D, respectively. Abbreviations: am-ampulla; bd-primary bud; zo-zooid. (e) qPCR analysis summarizing the global changes in IAP genes expressions along blastogenesis. Each blastogenetic stage is plotted versus the corresponding ΔC_T average of all tested IAP genes. Significant differences in comparison to blastogenetic stage A: *p < 0.05, **- p < 0.005 and significant difference from stage B: ***P < 0.0005. (f) Relative qPCR analysis of gene expressions along the blastogenetic cycle. The comparison is made between ramets originating from the same colony. Only tested genes that changed significantly along the blastogenetic cycle ($p_A < 0.05$) are shown. The fold change in genes expressions are relative to those at blastogenetic stage A and are presented at $\log_2$ scale. Significant differences in comparison to blastogenetic stage A: * p < 0.05, **- p < 0.005 and significant difference from stage B: *p < 0.05, **p < 0.005; ***p < 0.0005. (g) Relative qPCR analysis of tested genes expressions in *B. schlosseri's* various modules/colonial areas. Only statistically significant changes are presented. Gene quantity is expressed as fold change (at $\log_2$ scale) relative to zooidal tissue at blastogenetic stages C/D. The comparisons are between tissues extracted from the same colony (x5 biological repeats) and include zooids at blastogenetic stage C/D; buds at blastogenetic stage C/D; ampullae and tunic at blastogenetic stage C/D; Zooids at blastogenetic stage A; ampullae and tunic at blastogenetic stage A. p-values: *p < 0.05; **p < 0.005; ***p < 0.0005.

Table 1
IAP genes with significant altered expressions along the blastogenesis cycle.

Gene	ANOVA	P value of post pairwise comparisons					
	P_A value	AB	AC	AD	BC	BD	CD
IAP2	**0.001**	0.066	1.00	0.26	0.216	**0.026**	1.000
IAP6	**0.05**	0.087705	**0.003936**	0.09336	**0.037865**	**0.048697**	0.954269
IAP8	**0.00042**	1.000	0.055	**0.006**	**0.001**	**0.005**	0.046
IAP9	**0.004**	1.000	1.000	0.448	**0.042**	**0.00017**	1.000
IAP14	**0.031**	1.000	0.421	0.319	0.203	0.401	1.000
IAP16	**0.001**	1.000	**0.049**	0.076	0.094	0.165	1.000
IAP17	**0.011**	0.155	0.051	0.188	0.084	0.415	0.145
IAP18	**0.016**	1.000	**0.038**	**0.015**	0.537	1.000	0.222
IAP21	**0.00008**	1.000	**0.006**	**0.010**	**0.024**	**0.022**	0.566
IAP28	**0.0000066730**	1.000	**0.001**	**0.00045**	0.116	**0.011**	1.000
IAP41	**0.018**	1.000	1.000	0.0730	1.000	0.231	0.447
IAP42	**0.035**	1.000	1.000	0.521	**0.019**	**0.016**	1.000
AIF1	**0.012**	1.000	0.5250	0.1690	1.000	0.2940	0.0550
BAX	0.029	1.000	0.542	0.112	1.000	**0.007**	0.043
Mcl 1	0.018	0.761	1.000	0.616	0.321	**0.003**	1.000
Caspase 2	**0.030**	1.000	0.181	**0.024**	0.228	0.129	0.627
Caspase 7.1	**0.010**	1.000	0.095	0.240	**0.023**	0.082	1.000
Caspase 7.2	**0.002**	1.000	**0.017**	**0.023**	**0.009**	**0.002**	0.313

ANOVA repeated measures analysis of the results obtained following relative qPCR quantification of genes expressions at the four blastogenetic stages (A, B, C, and D). Only genes that are significantly changed at least in one of the stages are shown. P_A-value (p-value of ANOVA test) among the four blastogenetic stages and p-values, of the pairwise comparison (of the post-hoc analyses) are shown for tested genes that satisfied $P_A < 0.05$.

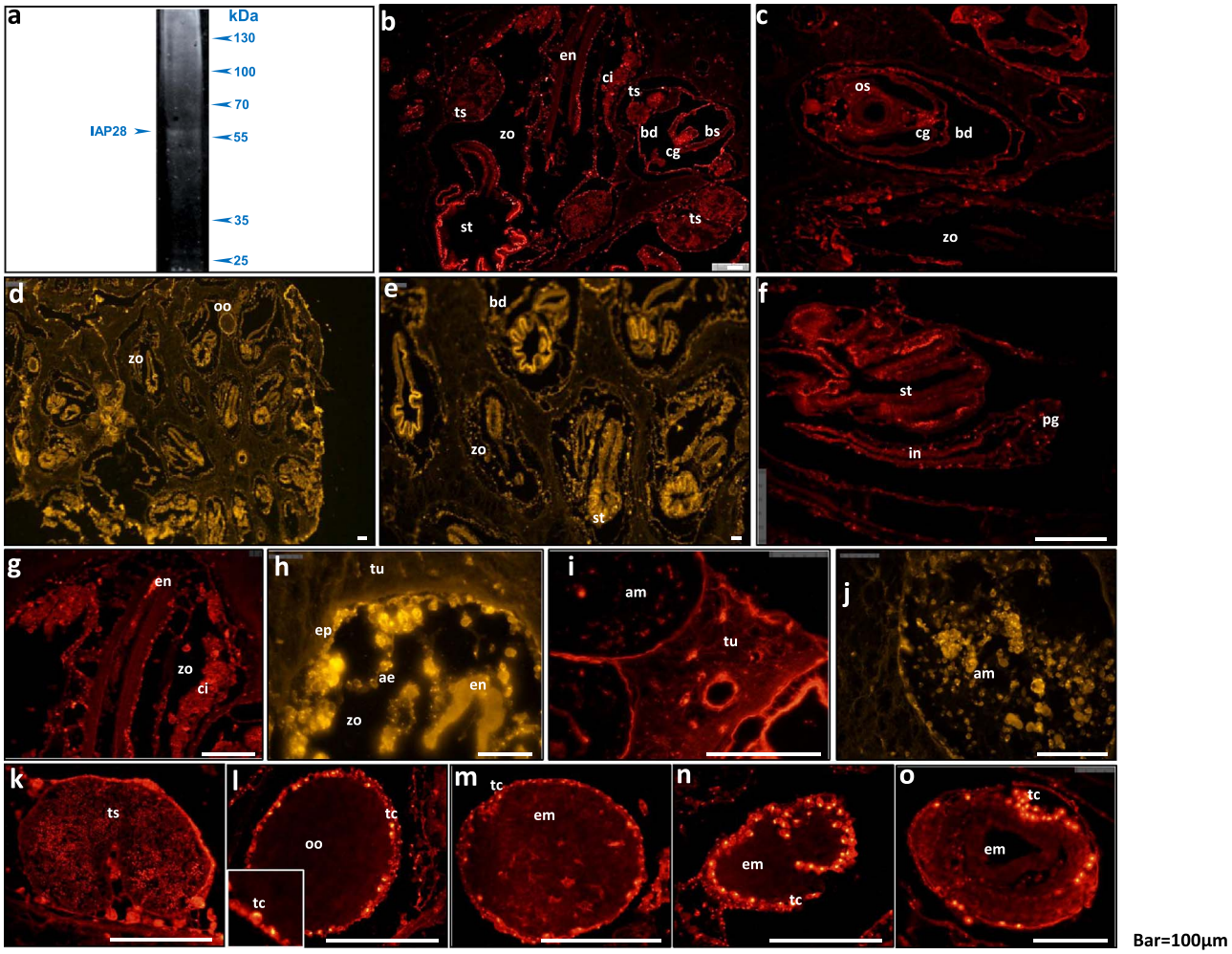

Fig. 3. Western and Immunohistochemical analyses of *B. schlosseri* sections with anti-IAP28 polyclonal antibodies. (a) Western blot analysis of *B. schlosseri* stage D zooids whole protein extracts; (b-o) Immunohistochemical analyses; Cy™5 (b-c, f, g, i, k-o) or Cy™3 (d, e, h, j) conjugated antibodies were used as secondary antibodies. The analyzed tissue include: (b) a section of a colony at stage B; (c) a section of a colony at stage C; (d-e) sections of a colony at stage D; (f) digestive tract region from a colony at stage A; (g) endostyle region from a colony at blastogenetic stage B; (h) an endostyle region from a colony at blastogenetic stage D; (i) tunic matrix from a colony at blastogenetic stage D; (j) an ampulla from a colony at blastogenetic stage D; (k) a testis from a colony at blastogenetic stage B; (l) an egg. The white box contains magnification of the cell layers (follicular and test cells) that are wrapping the egg; (m-o) young embryos at various developmental stages. Abbreviations: ae-atrial epithelium (peribranchial epithelium); am-ampulla; bd- primary bud; bs-branchial sac; cg-central ganglion; ci-cell island; em-embryo; en-endostyle; ep- epidermis; in- intestine; oo-oocyte; os-oral siphon; st-stomach; tc-test cells; ts-testis; tu-tunic; zo-zooid. Bar = 100 µm.

during stage D, the IAP28 expressions increased in the buds, mainly in the stomach (Fig. 3d, e). In blastogenetic stage D zooids, we documented increased staining in macrophage-like phagocytic cells that are dispersed in the zooids (Fig. 3e). Strong staining was detected in cell populations loosely connected to the atrial epithelium (Fig. 3h), circulating blood cells and in cells at the cerebral ganglions. Mild increase in IAP28 expression is detected in the branchial sacs (Fig. 3e). The ampullae of colonies at blastogenetic stage D are heavily populated with IAP28 positive cells (Fig. 3j), primarily in aggregated and dispersed 5 µM cells. IAP28 also stains male gonads (Fig. 3k), test cells that are wrapping oocytes (Fig. 3l), and test cells in the tunics that wrap embryos at various developmental stages (Fig. 3m-o). We further observed some sporadic staining in embryos (Fig. 3m, o), yet significantly weaker than in the test cells.

3.3. Apoptosis induction by H_2O_2

IAP genes function in many processes other than Apoptosis. The next set of experiments were designed to artificially induce apoptosis in blastogenetic stage A colonies in order to identify IAP genes that are specifically associated with apoptosis. Nineteen *B. schlosseri* colonies at blastogenetic stage A were submerged for 20–24 h in 100 µM H_2O_2 (apoptosis inducing level) or in 1000 µM H_2O_2 (necroptosis inducing level; J. Xiang et al., 2016), while genetically matched controls were submersed in clean seawater. Treatments with 100 µM H_2O_2 did not affect morphologies (Fig. 4a), while the 1000 µM H_2O_2 treatment resulted in shrunken zooids, buds and ampullae, loosening of the common exhalant siphon, increased pigmentation and other stress related phenotypes (Fig. 4b) as already described in Rosner et al. (2007).

For qPCR, we used five sets of 1000 µM H_2O_2 treated ramets and their controls, and four sets of 100 µM H_2O_2 treated ramets and their controls. Genes analyzed included IAP genes (besides IAPs 40–43), AIF1, caspase 2, caspase 3, caspase 9 and two gene homologous to caspase 7 (marked as 7.1 and 7.2). Significance was tested by paired *t*-test for each concentration of H_2O_2 separately. Significant increased expressions (Fig. 4c) were revealed for AIF1, Caspases 7.1 and Caspase 9 in response to 100 µM H_2O_2 but not to 1000 µM H_2O_2. Four IAP genes (IAP6, IAP14, IAP21 and IAP28) that are active in blastogenesis, were also upregulated during treatment in both H_2O_2 concentrations. Two genes (IAP 9 and IAP 16) are involved in blastogenesis but were not affected in the H_2O_2 treatments. Two genes (IAP8 and IAP18) are active in blastogenesis and were upregulated in the 1000 µM H_2O_2 administration; one gene (IAP15) was upregulated in both H_2O_2

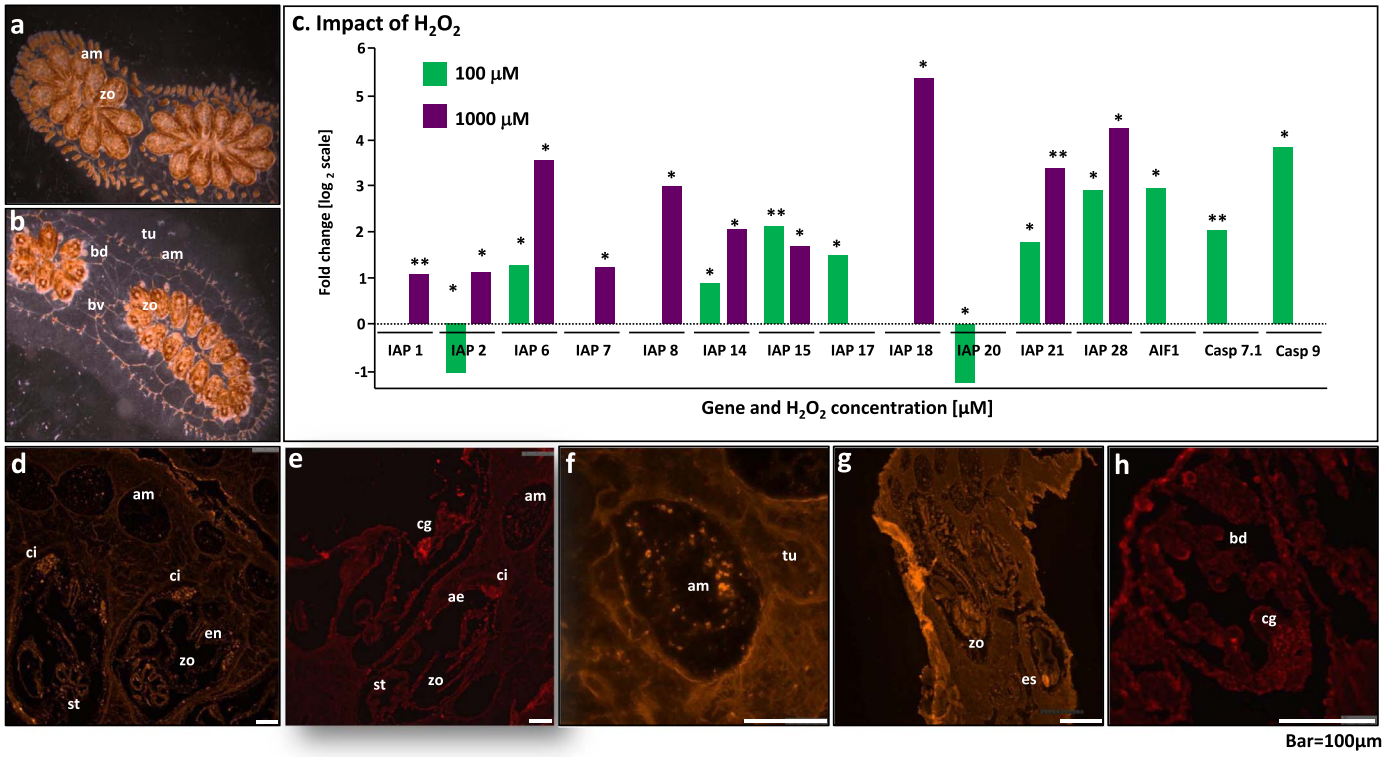

Fig. 4. Impacts of the administration of 100 µM H_2O_2 or 1000 µM of H_2O_2 on *B. schlosseri* colonies. (a) colony phenotype following treatment with 100 µM H_2O_2; (b) colony phenotype following treatment with 1000 µM H_2O_2; (c) relative qPCR analyses for IAPs, AF1 and caspases expressions following administration of 100 µM H_2O_2 (green bars) or 1000 µM H_2O_2 (purple bars) relative to controls that were submerged in clean seawater. All colonies were at blastogenetic stage A at onset. The figure summarizes only statistically significant changes in gene expressions. Gene expressions are presented as fold changes (at log2 scale) relative to control colonies at blastogenetic stage A. p-values: * $p < 0.05$; **$p < 0.005$. (d-h) Immunohistochemical analyses of colonies treated with (d-f) 100 µM H_2O_2 or (g, h) 1000 µM. H_2O_2 and stained with anti-IAP28 antibodies. Cy™5 (e, h) or Cy™3 (d, f, g) conjugated antibodies were used as secondary antibodies. The panel contains pictures of (d,e) zooids of a blastogenetic stage A colony; (f) an ampulla from a blastogenetic stage A colony; (g) a colony at blastogenetic stage A; (h) a bud from a colony at blastogenetic stage B. Abbreviations: ae-atrial epithelium; am-ampulla; bd- primary bud; bv-blood vessel; cg-central ganglion; ci-cell island; en-endostyle; st-stomach; tu-tunic; zo-zooid. Bar = 100 µm.

treatments, but not in blastogenesis; IAP1 was upregulated following 1000 µM H_2O_2 treatment and IAP2 and IAP20 were down-regulated following 100 µM H_2O_2 administration. Altogether, results suggest that at least five of the genes (IAP6, IAP14, IAP17, IAP21 and IAP28) that were upregulated towards the takeover phase of the blastogenetic cycle, might function in processes related to apoptosis.

We further employed immunohistochemical analyses to identify IAP28 expressions following H_2O_2 administrations (Fig. 4d-h). IAP28 staining after submersion of colonies in 100 µM H_2O_2 was detected in the blood cells and phagocytes in the CI and in scattered cells all over the zooids (Fig. 4d). Staining was also detected in the cerebral ganglion (Fig. 4e) and in blood cells within the ampullae (Fig. 4f). In the 1000 µM H_2O_2 treatment, staining was detected in the pharynx and the stomach (Fig. 4g) and in the neural system of the developing buds and in the zooids (Fig. 4h). These results further indicate a possible link between apoptosis, IAP28 and phagocytes population.

3.4. Impacts of Smac mimetic drugs on the blastogenetic cycle

Smac mimetic drugs like GDC-0152 were developed for the treatment of solid tumors and hematologic cancers. GDC-0152 induces apoptotic death of cancer cells by down-regulating expressions of the IAPs, PI3K and Akt (Hu et al., 2015). Here we used Smac mimetic drugs to evaluate how impairment of IAP gene functions affects the phenotype of the colony and the takeover process. Five colonies at blastogenetic stage A (designated A1-A5), and five colonies at blastogenetic stage C or D (designated D6-D10) were submerged in seawater containing 2 mg/liter of GDC-0152 dissolved in DMSO, while controls were submerged in seawater containing DMSO without an the inhibitor. Seawater was exchanged after one week and a fresh dose of GDC-0152 and control DMSO, respectively, were added. The colonies were observed daily for two weeks. Deformations occurred in nine of the ten colonies tested (Fig. 5a-f). Zooids in colonies A3 (Fig. 5a) and D6 (Fig. 5b) started to shrink one day after the GDC-0152 administration, and thereafter they deteriorated. Colony D6 revealed lethargic growth of the buds while starting the new blastogenetic cycle, and during the next 12 days this colony did not complete the blastogenetic cycle. For the rest 7 colonies the blastogenetic cycle was shortened to five days while inducing morphological malformations before and during, the takeover stage. These malformations include reductions in size and bud growth rates, colonies containing primary buds of different sizes (5 colonies; Fig. 5b, c, d), increased pigmentation (Fig. 5a, two colonies), disruption of normal colonial architectures (7 colonies; Fig. 5a-c, f), unsynchronized blastogenesis (3 colonies; Fig. 5e), contraction and pigmentation of ampullae (3 colonies; Fig. 5b, c, f) and shrinkage of zooids (3 colonies; Fig. 5b, d). The small-undeveloped buds were absorbed together with the zooids during the takeover phase, thus colonial sizes were reduced.

RNA was extracted from the deformed colonies for qPCR analyses, using the same battery of genes (five blastogenetic stage A treated colonies and four stage D treated colonies were compared to corresponding controls). In stage A colonies, while Myc, Sox2, Pl10 and β-catenin mRNA levels remained steady following treatment (data not shown), significant increase in mRNA expressions was recorded for the apoptotic regulator Mcl1 and caspase 9 genes (Fig. 5g; purple bars), in accordance with results by Hu et al. (2015). Increased expressions of 16 IAP genes and of Akt were further detected apparently opposed to results by Hu et al. (2015). Among IAPs, IAP14 was the most affected gene with a 7.67 fold increase (Fig. 5g). The nine IAP genes not altered under GDC-0152 treatment included IAP8, IAP9, IAP16, IAP21 and IAP28, genes that were highly associated with the takeover stage, of

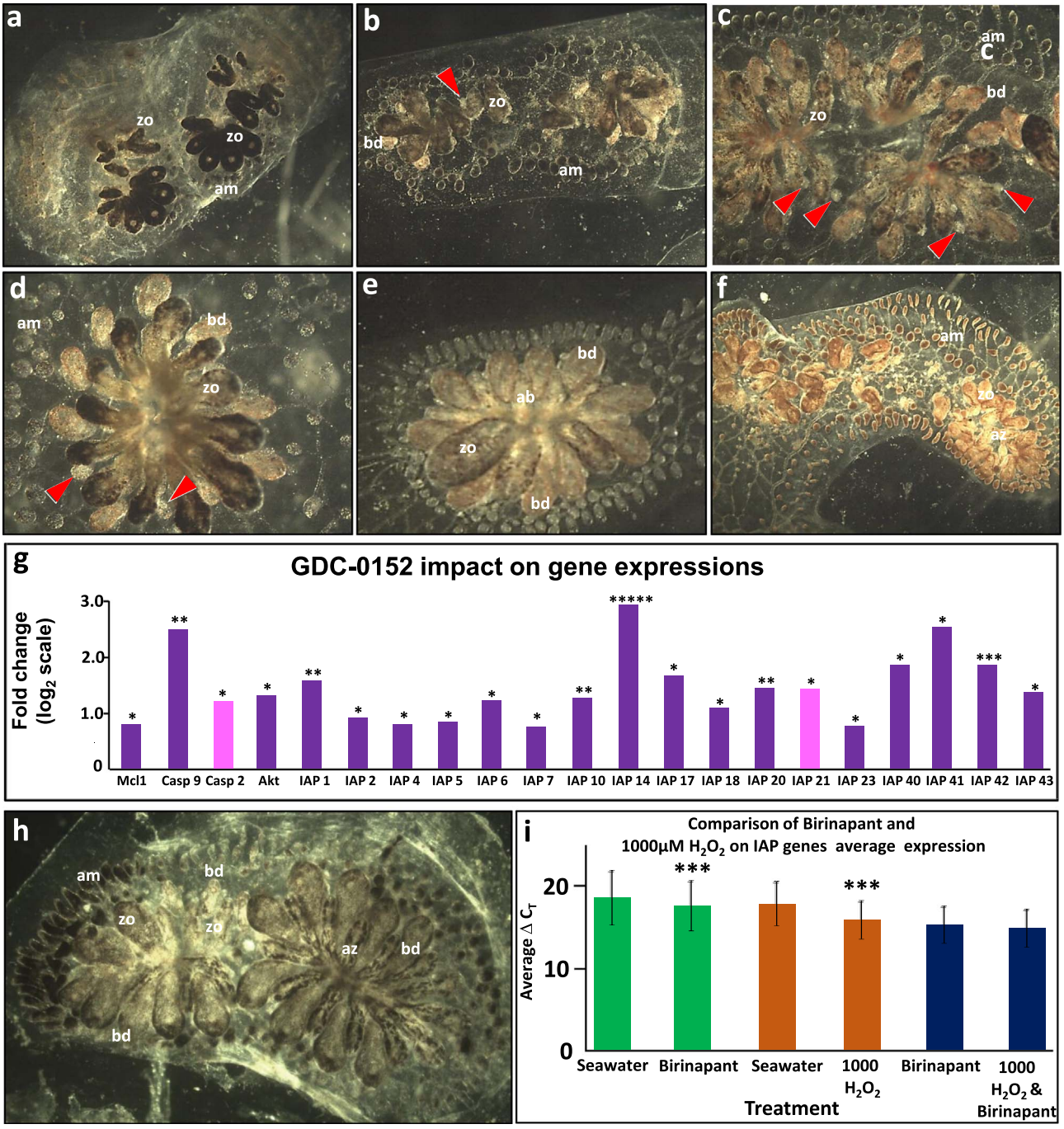

Fig. 5. Impacts of Smac mimetic drugs on the blastogenetic cycle. (a-f) Impacts of GDC-0152 on the *B. schlosseri* morphology at different stages of the blastogenetic cycle including (c, e, f) the takeover phase. Red arrowheads point to small underdeveloped buds; Abbreviations: ab-absorbed zooid; am-ampulla; bd- primary bud; zo-zooid; (g) qPCR analyses revealing significant changes of IAP and apoptosis related genes expressions following the addition of 2 μg/ml GDC-0152. Comparisons were made between blastogenetic stage A treated colonies and controls at the same blastogenetic stage (purple bars) or blastogenetic stage D treated colonies and controls at the same blastogenetic stage (pink bars). Only genes with significant expression change are shown. p-values: * $p < 0.05$; ** $p < 0.005$; *** $p < 0.0005$; ***** $p < 0.000005$; (h) Impact of Birinapant on colony morphology. (i) Birinapant and 1000 μM H_2O_2 impacts on IAP gene global expressions as revealed by qPCR analyses. The average ΔC_T of all IAP genes in each treatment is plotted versus the average ΔC_T of all IAP genes in the respective control. (i, green bars) significant differences between IAP genes expressions in blastogenetic stage A colonies treated with Birinapant and controls at stage A. (i, orange bars) significant differences between IAP genes expressions in blastogenetic stage A colonies treated with 1000 μM H_2O_2 and controls at blastogenetic stage A. (i, blue bars) No expressions differences between tissues treated with Biriniapnt alone relative to tissue treated with Birinapant and immediately afterwards with 1000 μM H_2O_2. p-value: ***$p < 0.0005$.

which IAP8, IAP21 and IAP28 are also associated with apoptosis and necroptosis. Blastogenetic stage D GDC-0152 treated colonies revealed increased expressions in only two of the genes: caspase 2 and IAP21 (Fig. 5g, pink bars).

We further used Birinapant, a Smac mimetic IAP antagonist (not for all IAP genes; Krepler et al., 2013) on 19 colonies. Colonies were submerged in seawater containing 1.1 mg/liter of Birinapant dissolved in DMSO, or DMSO only as control. In contrast to the GDC-0152 treatment, morphological changes were detected only in one out of the 19 tested colonies (Fig. 5h), in accordance with Birinapant's modest results during *in vivo* trials (Finlay et al., 2017). No significant changes were observed in caspase mRNA expressions. Since clinical trials revealed synergistic results with Birinapant and an additional anti cancerous agent (Krepler et al., 2013), we searched here for similar outcomes using Birinapant and 1000 μM H_2O_2. Indeed, qPCR analyses revealed significant increase in the average of IAP genes expressions in

treated blastogenetic stage A colonies as compared to stage A controls, as occurred following treatment with GDC-0152 (Fig. 5i, green bars), as well as in treatments with 1000 μM H_2O_2 (Fig. 5i, orange bars). However, comparisons between both experiments showed no additive or synergistic expression (Fig. 5i, blue bars).

3.5. Budectomy and whole body regeneration

Previous studies (Lauzon et al., 2002) demonstrated an interplay and crosstalk between buds and zooids, significantly regulating the takeover process. Surgically removing all buds (budectomy) demonstrated that the onset of apoptosis was independent of the existence of buds. However, the resorption of zooids was linked to the presentence of buds, as a single functional bud in the colony resulted in delayed absorption of the old generation of zooids (48–60 h instead of 24–36 h). In light of these results, we conducted a series of experiments aimed to clarify the role of IAP genes during budectomy, and thus to understand their function during turnover. Budectomy was performed on 31 *B. schlosseri* colonies, and outcomes were compared to respective intact controls. The impacts of budectomy were analyzed by three sets of analyses: (a) Phenotypic changes that were monitored daily for 28 days (n = 11, Fig. 6a and Table 2); (b) Immunohistochemical analyses using anti-Pl10 antibodies that stain differentiating tissues and phagocytic cells, anti-Vasa antibodies that stain cells of the germ lineage, and anti-pH3 antibodies that stain dividing cells. These three antibodies marked living cells and tissues and assisted in the interpretation of the staining obtained with anti-IAP28 antibodies (n = 11, Fig. 6b); (C) qPCR analyses of IAP and selected pro-survival and control genes (n = 9, Fig. 6c, d).

Not a single phenotypic change was observed in the first few days following budectomy. First morphological changes in budectomized fragments were initiated only at blastogenetic stage D. While zooids in the control ramets proceeded with normal absorption and takeover processes, budectomized ramets started blastogenetic stage D as controls (Lauzon et al., 2002), but then the absorption course was interrupted, leading to a series of morphological changes that were culminated with the formation of new zooids. Fig. 6a and Table 2 (28 observational days) detail a series of seven phenotypic steps that developed in each one of the 11 budectomized ramets. These include: (1) the appearance of giant, sausage-like ampullae loaded with blood cells, including pigment cells (Fig. 6a1,2); (2) chaotic morphologies of aggregated and partially damaged zooids with dilated ampullae that may overlap the zooidal remains (Fig. 6a3); (3) development of one to several regeneration centers, first appearing as transparent shiny 'bubbles' (Fig. 6a4); (4) The 'bubbles' differentiation into zooids (Fig. 6a5, 6); (5) maturation of the newly formed zooids (Fig. 6a7); (6) the formation of the first 'system' (Fig. 6a8); (7) clearance of absorbed zooidal remains and the recovery of the normal ampullar phenotype (Fig. 6a8). All budectomized ramets succeeded to produce at least one zooid per ramet, 10–13 days following budectomy (Table 2). However, many of the ramets did not succeed to complete additional blastogenetic cycles as 36.4% of the ramets died within one month following budectomy, while their controls survived. At 7 weeks following budectomy, an additional portion (27.3%) of the regenerating ramets died simultaneously with their controls, indicating that these added mortalities were probably caused by malady or by their programmed life span (Rinkevich et al., 1992).

Immunohistochemical analyses of budectomized ramets at the various stages of regeneration are shown on Fig. 6b. Surprisingly, anti-pH3 antibodies staining indicated cell proliferation at early blastogenetic stage D budectomized colonies (Fig. 6b1) and differentiating rudiment tissues were stained with anti-pH3 and ani-Pl10 antibodies (Fig. 6b2, 3, respectively), but not with anti-IAP28 antibodies (Fig. 6b4). Anti-IAP28 antibodies stained zooidal atrial epithelium and a few sporadic phagocytic cells scattered all over the colony (Fig. 6b4). Phagocytic activity of macrophage-like cells, stained with ani-Pl10 antibodies, was also detected within the zooids (Fig. 6b5) for a short period, and then disappeared following the next stages of regeneration (as from the formation of the regeneration centers; Fig. 6b6). Immunohistochemical analyses of sections from the 'regeneration centers' stage (Fig. 6b6–13), revealed new staining of Pl10 in these centers (Fig. 6b6, 7), in which the emerging internal organs (endostyle, branchial sac and digestive tissue; Fig. 6b8) developed abnormal morphologies. Some of the developing zooids were attached to primary buds (Fig. 6b7, 8) that were populated with Vasa positive germ cells (Fig. 6b8). PL10+ pH3+ 'regeneration centers' were initiated from absorbed zooids and ampullae (Fig. 6b9,10,11) but were not stained with anti-IAP28 antibodies. All along the 'regeneration centers' stage IAP28 staining was very low, and was found only in few sporadic blood cells (Fig. 6b12) and in the zooidal atrial epithelium (Fig. 6b13). In this stage, phagocytes were not stained by ant-IAP28 nor by ant-PL10 antibodies. In the next developmental stages, the zooids became opaque with opened siphons. Remains of the old zooids and dark enlarged ampullae were interlaced between the newly formed zooids (Fig. 6a7). Immunohistochemical analyses revealed high proliferative activity ($pH3^+$) in differentiating buds (Fig. 6b14) and large numbers of $IAP28^+Pl10^+$ phagocytic cells (Fig. 6b15, 16). After a couple of blastogenetic cycles, the colony regained its normal appearance and tissue organization, as revealed by the immunochemistry (Fig. 6b17, 18).

Two sets of qPCR experiments were performed. They analyzed gene expressions in budectomized ramets, a few hours following the closure of the siphons (four biological repeats) as compared to stage D control ramets (Fig. 6c and d, green bars), and gene expressions of budectomized ramets (five biological repeats) compared to naïve controls, when controls entered the following blastogenetic stage A (Fig. 6c and d, red bars). Analyses revealed significant increase in IAP genes global expressions in budectomized ramets relative to stage D controls (Fig. 6c, green bar) and to stage A controls (Fig. 6c, red bar). As expected, genes like Sox2 and Myc, which are highly expressed in buds, were significantly down regulated in budectomized stage D ramets (Fig. 6d). The upregulated transcription of Hsp90β and of the pro-survival PI3K/Akt pathway genes (Akt, Pik3ca; Fig. 6d) are in accordance with expected results, but the simultaneous upregulation of Gsk3b is confusing, since this gene is normally down regulated by the PI3K/Akt pathway. In addition, while Pl10 expression in budectomized ramets is expected to be reduced (because of high expressions in buds), it was upregulated (Fig., 6d). The expressions of 12 IAP genes were significantly changed (Fig. 6d), 5 of which (IAPs 8, 14, 16, 28, 41) already recorded by increased expressions in normal blastogenetic stage D colonies (Fig. 2f). In contrast, IAP9 and IAP15 enhanced expression in buds (Fig. 2g) can be the source for the down-regulation in budectomized ramets. In summary, IAP genes, specifically associated with whole body regeneration following budectomy, include IAP2, IAP10, IAP13 and IAP14 (also associated with blastogenetic stage D) all of them were upregulated in budectomized ramets relative to blastogenetic stages D and A controls. IAP1 and IAP42 are upregulated only relative to stage A.

3.6. The sway on budectomy

We studied the restraint of buds on whole body regeneration phenomenon, in a variant of partially-budectomized (termed as hemi-budectomized) colonies, following previously described experiments (Lauzon et al., 2002). Our experiments were performed on colonies composed of two systems; in these colonies, all vasculature connecting the two systems were experimentally removed except for a single blood vessel that was left intact. One of the systems was budectomized while the second system was left unharmed, an experimental manipulation called Bct (Budectomized & **c**onnec**t**ed) ramets (Fig. 7a,b). Ten Bct assays were observed daily for morphological changes (Table 3), revealing disparate developmental outcomes from budectomized ramets. In 8 of the 10 Bct assays, all zooids were absorbed within 7–11 days following the procedure (depending on the blastogenetic stage at budectomy). In the other two cases the single connecting blood vessel was also detached (Table 3, P3, P8). In assay

P3 the connective blood vessel deteriorated one day after budectomy and the budectomized system was regenerated, while in P8 the connecting blood vessel deteriorated after 14 days and the budectomized system did not regenerate.

While regenerating budectomized ramets (Bz; Fig. 7, ramet c) showed dark enlarged ampullae and centrally retracted zooids with closed siphons, Bct assays (Fig. 7, ramet b) showed light-colored ampullae and significantly smaller and brighter zooids. We performed immunohistochemical analyses on these Bz and Bct ramets using anti-pH3, anti-Vasa, anti-Pl10 and anti-IAP28 antibodies at the stage where corresponding control ramets reached blastogenetic stage A (Fig. 7, ramet a). The analyses of Bct ramets revealed muddled morphology of

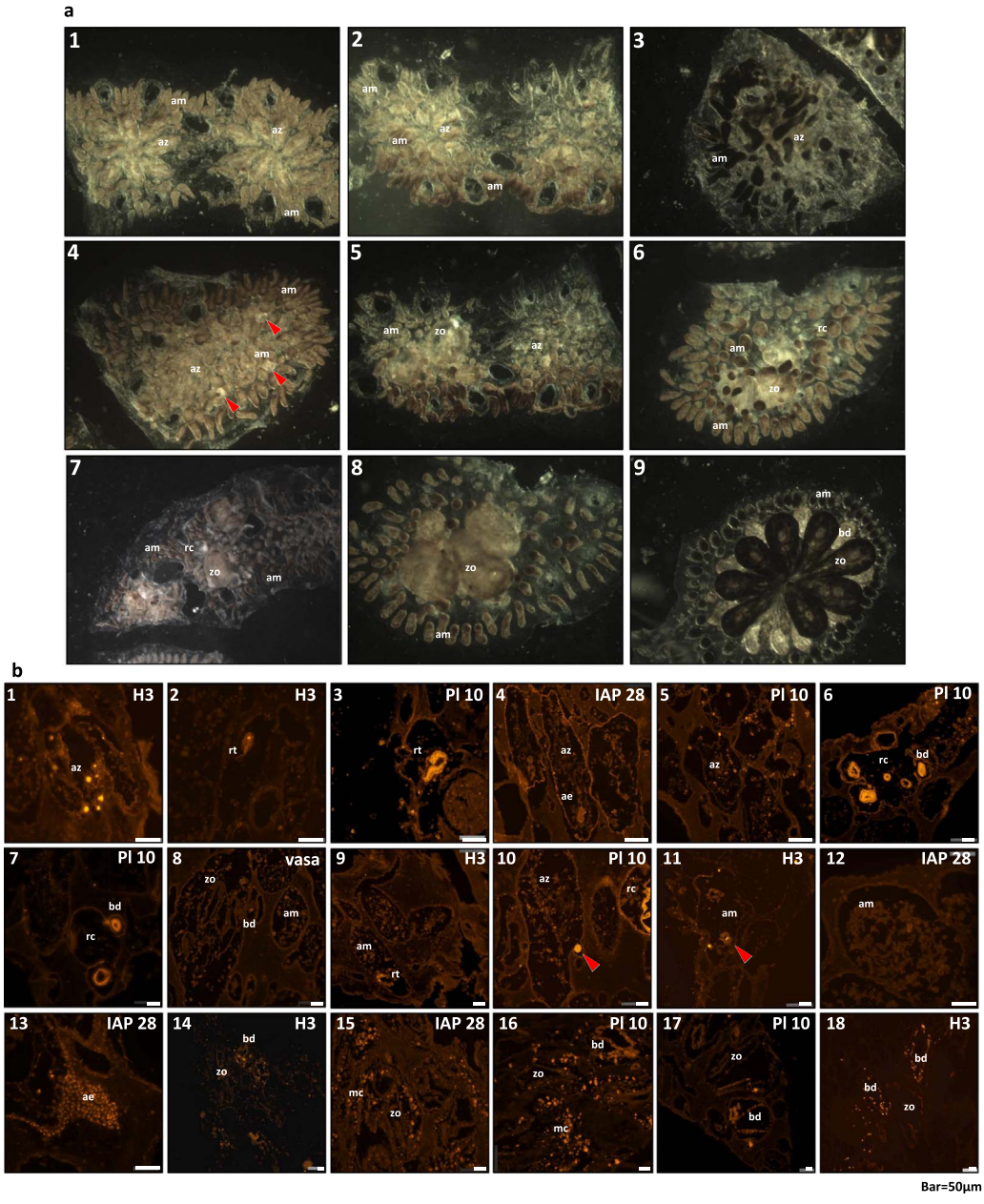

Fig. 6. (a) Budectomy induced whole body regeneration. The various steps from removal of the buds until the formation of the single system colony are shown. (1) Deformation of ampullae; (2) Condensation of the partially absorbed zooids in the center of the colony; (3) Chaotic arrangement of zooids tightly condensed with large black ampullae that are interlaced between and above the zooids; (4) Appearance of transparent 'regeneration centers'. Arrowheads point to foci of regeneration. (5) Formation of a zooid; (6) Sometimes, more than a single zooid is formed; (7) The zooids open their siphons; (8) Remains of the old generation of zooids are removed, ampullae regain normal phenotype, a pseudo 'normal' system is formed; (9) A morphologically regular colony is formed with a single colonial system. (b) Immunohistochemical analyses of budectomized tissues at the various steps of regeneration with anti-IAP28, anti-pH3, anti-Pl10 and anti-Vasa antibodies. Anti-Pl10 antibodies stain differentiating tissue (buds, germ cells) and phagocytes (Rosner et al., 2006). Anti-pH3 antibodies specifically stain nuclei of cells during mitosis or meiosis. Anti-Vasa antibodies stain the cells of the germ lineage. (1) Budectomized colony a few hours following siphon closure; (2–5) Ramets from the 'chaotic' morphology of early regeneration; (6–13) Ramets from the 'regeneration centers' step; (14–16) Ramets from the 'siphon opening' stage; (17–18) Ramets after full recovery. Abbreviations: ae- atrial epithelium; ab-absorbed zooid; am-ampulla; mc-macrophage-like cell; bd-primary bud; rc-regeneration center; rt-regenerating tissue; zo-zooid. Bar-50 µm; Red arrowheads point to regenerating tissues. (c, d) qPCR quantification of genes in budectomized *B. schlosseri* colonies analyzed by paired *t*-test. Two sets of experiments were performed. One set revealed the expression changes of budectomized ramets few hours after zooidal siphons closure (early blastogenetic stage D) relative to control colonies at blastogenetic stage D (green bars). The other set revealed expression changes one day afterwards, when control ramets started a new blastogenetic cycle and (red bars). (c) Global changes of IAP genes expressions presented by comparing the average ΔC_T of all IAP genes in budectomized tissues versus their respective controls; (d) Expressions of genes that were tested and found to be significantly altered following budectomy as fold change relative to their respective controls (at $\log_2$ scale). p-values: *$p < 0.05$; ** $p < 0.005$; *** - $p < 0.0005$; **** $p < 0.00005$; ***** $p < 0.000005$.

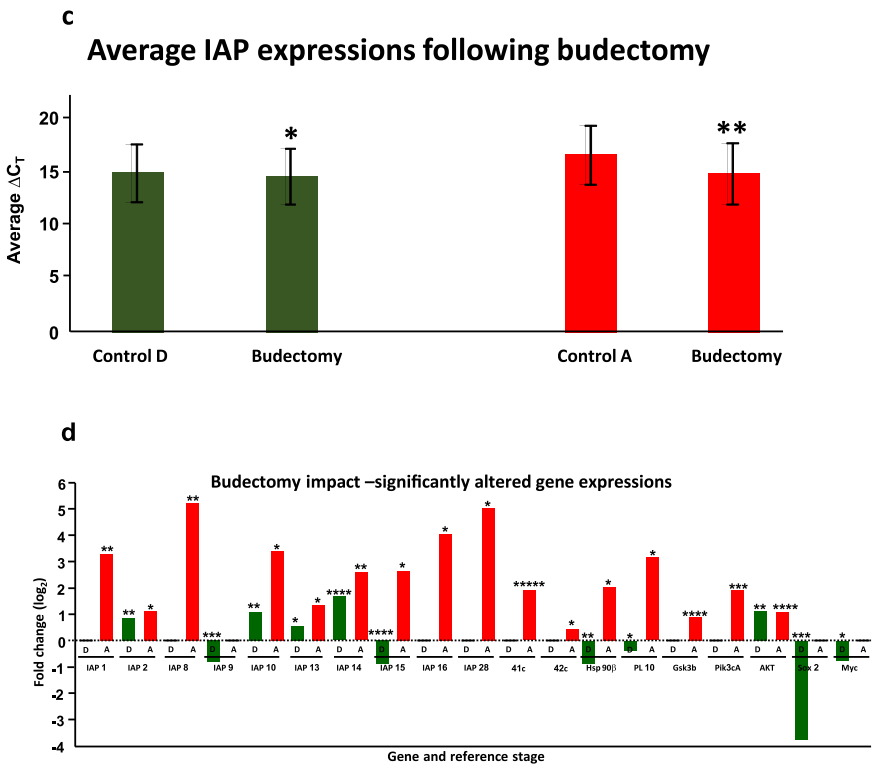

Fig. 6. (*continued*)

shrunken zooidal organs, with barely detected IAP28 staining in a few cells (Fig. 7b1). Sporadic staining with anti-pH3 antibodies was detected in ampullar endothelium and in the zooids (Fig. 7b2), while tightly packed (Rosner et al., 2013) large numbers of Vasa positive oocytes and other germ lineage cells were detected in ampullae and in the remains of absorbed zooids (Fig. 7b3). As absorption of the zooids advances, the H3 and Vasa staining disappear. The last staining of Pl10$^+$ Vasa$^+$ cells (Fig. 7b4) was detected in 5–6 μm ampular cells that contained large nuclei (Fig. 7b4). In Bz assays zooidal remains were located contemporaneously to the sites of early centers of regeneration (Fig. 7c1, red arrows), that were PL10$^+$ and H3$^+$ (Fig. 7c2), but IAP28$^-$ (Fig. 7c1). The positive H3 staining was significantly higher than in Bct tissues and also included, beside the regenerating tissues, cells in the zooids along the ampullar endothelium. The regenerating budectomized tissue, like the Bct tissue, contained large aggregates of Vasa$^+$ and Pl10$^+$ cells (Fig. 7c3 and 4).

Using qPCR we further compared gene expressions in three situations: 'normal' (intact blastogenetic stage A controls in which buds were removed just before RNA extractions), Bz and Bct (Fig. 7a,b,c). Comparison of average ΔC_Ts of IAP genes in these three situations revealed that IAP genes are significantly up regulated in Bz colonies in comparison to both 'normal' and Bct colonies (Fig. 7d). Genes with significant expression changes in four biological repeats are shown in Fig. 7e. IAP14 and IAP4 expressions in Bz colonies are specifically elevated relative to both 'normal' and Bct. As in a previous experiment (Fig. 6d), genes of the PI3K/Akt pathway were also upregulated. The last experiments reveal that IAP4 and IAP14 and the pro survival PI3K/Akt pathway are upregulated in concert with the budectomy induced regeneration.

3.7. Impact of Smac mimetic drugs on budectomy induces regeneration

Fifteen colonies at various blastogenetic stages were each split into two halves on a single glass slide. One half was then budectomized and marked as Bz and the second remained intact and served as control. The slides were numbered and arbitrarily placed in three tanks. Seawater in tank no 1 was supplemented with 1 mg/l GDC-0152 dissolved in 100 μl/l of DMSO (enabling prolonged exposures), the seawater in tank no 2 was supplemented with 1.1 mg/l Birinapant dissolved in 100 μl/l DMSO, and in tank no 3 supplemented with 100 μl/l DMSO. The water and chemicals were replaced every other day. The intact halves were then budectomized on day 9 and marked with the suffix 'bis'. On day 11 all slides were transferred to clean seawater tanks and were observed daily for one month totally (Table 4-impacts of GDC-0152 administration; Table 5-impacts of Birinapant administration; Table 6-DMSO administration). Similarly to the previous experiment performed on whole colonies (Table 2), administration of Birinapant had no morphological impacts and 80% of the ramets regenerated at least one zooid followed by 40% mortality within the first month. GDC-0152 inhibitory effects were manifested on the bis ramets (Table 4), where neither one of the colonies regenerated a zooid and 80% died within one month.

3.8. Zooidectomy

As demonstrated here in previous sections, some of the IAP genes were up regulated in buds. Several of these IAPs might function in differentiation/proliferation processes intrinsically related to the buds, while other might be in response to signals coming from the zooids. As previously demonstrated, buds are capable to complete differentiation, takeover and transform into zooids in the absence of the old generation of zooid (Lauzon et al., 2002; Rosner et al., 2006). Therefore, we use zooidectomy (complete removal of the zooids) to distinguish between these options.

Each of the five colonies at blastogenetic stage A or B were surgically cut into two halves. One half served as control and in the second, all zooids were excised (Fig. 8). Similarly, to Rosner et al. (2006), zooidectomy was not followed by deterioration of the impacted ramets. Active ampullae continued to function in the periphery of the ramets (Fig. 8b, c) and the buds followed their normal blastogenetic route, where most of them completed differentiation into functional

Table 2
Regeneration of *B. schlosseri* budectomized colonies.

Day / Genet	0	1	2	4	4	5	6	7	8	9	10	13	14	16	17	20	23	24	28	105
B2	C	C	C	D	A	A	A	B	C	C	D	B	C	C	C	B	C	*	*	A
B4	B	B	C	C/D	A	A	A	B	C	D	A	C	C	A	A	C		*	*	
B6	C	C	D	A	B	B	B	C	D	A	A	C	D	A	A	C	B	C	C	B
B10	A	B	C	C	D	A	A	B	C	C	D	A	B	C / D	A	B	A	C	A	
B12A	B	B	C	D	A	B	B	B	C	D	A	A	C	A	B	C				
B12B	B	C	C	C	A	B	B	C	C	C	D	B	C	C / D	A	C	D		*	
B13	B	B	C	A		B	B	C	C	D	A	B	C	A	A	C	A	C	A	
B14	A	B	B	C	D	A	A	B	C	C	D	B	C	D	A	C	A	C	A	C
B15	B	B	C	C	D	A	A	A	B	B	B	C	A	A	C	A	B	A	C	
B18	B	B	C	C	D	A	B	B	C	C	D	A	B	C	D	A	C / D	B		
B20	C	C	C	D	A	A	A	B	C	C	A	A	C	D / A	A	B	A	B		A

A, B, C, D represent different blastogenetic stages of the control colony. * -represents stress of the control.

- Normal phenotype
- Giant ampullae loaded with blood cells
- Chaos stage-tightly packed zooids and ampullae
- Appearance of regeneration centers
- Formation of zooids
- Zooids with open syphons
- Formation of a first 'system'
- Clearance of remains of old zooid and return to normal phenotype
- Colonial death

Daily follow-up on whole body regeneration of budectomized colonies (Bz; n=11). The observed outcomes are marked by different colors, denoted in the table along with the blastogenetic stages of the genetically matched controls (labelled as A-D). Survivorship of the colonies was tracked for up to 7 weeks (105 days) following budectomy (budectomy = day 0).

zooids (Fig. 8d) at about the same time as their matched controls (within a couple of hours of delay, at most). Then, we measured the 25 IAP mRNAs levels between zooidectomized ramets (before development of new zooids) and their blastogenetic stage D controls. Expressions of only six genes (IAP1, IAP5, IAP8, IAP15, IAP18, IAP28) were significantly changed, unlike the change following budectomy. We recorded a significant increase in IAP15 and a decrease in IAP28 mRNAs, mimicking the normal expression patterns of these genes in buds and zooids, respectively (Fig. 2g), and enhanced mRNAs of IAP1, IAP5, IAP8 and IAP18. Upregulation of IAP8, previously associated with stage D zooids, is unexpected. These later changes can be attributed to the manipulation and the loss of zooidal control or to processes associated with the transition of the colony from stage D to stage A.

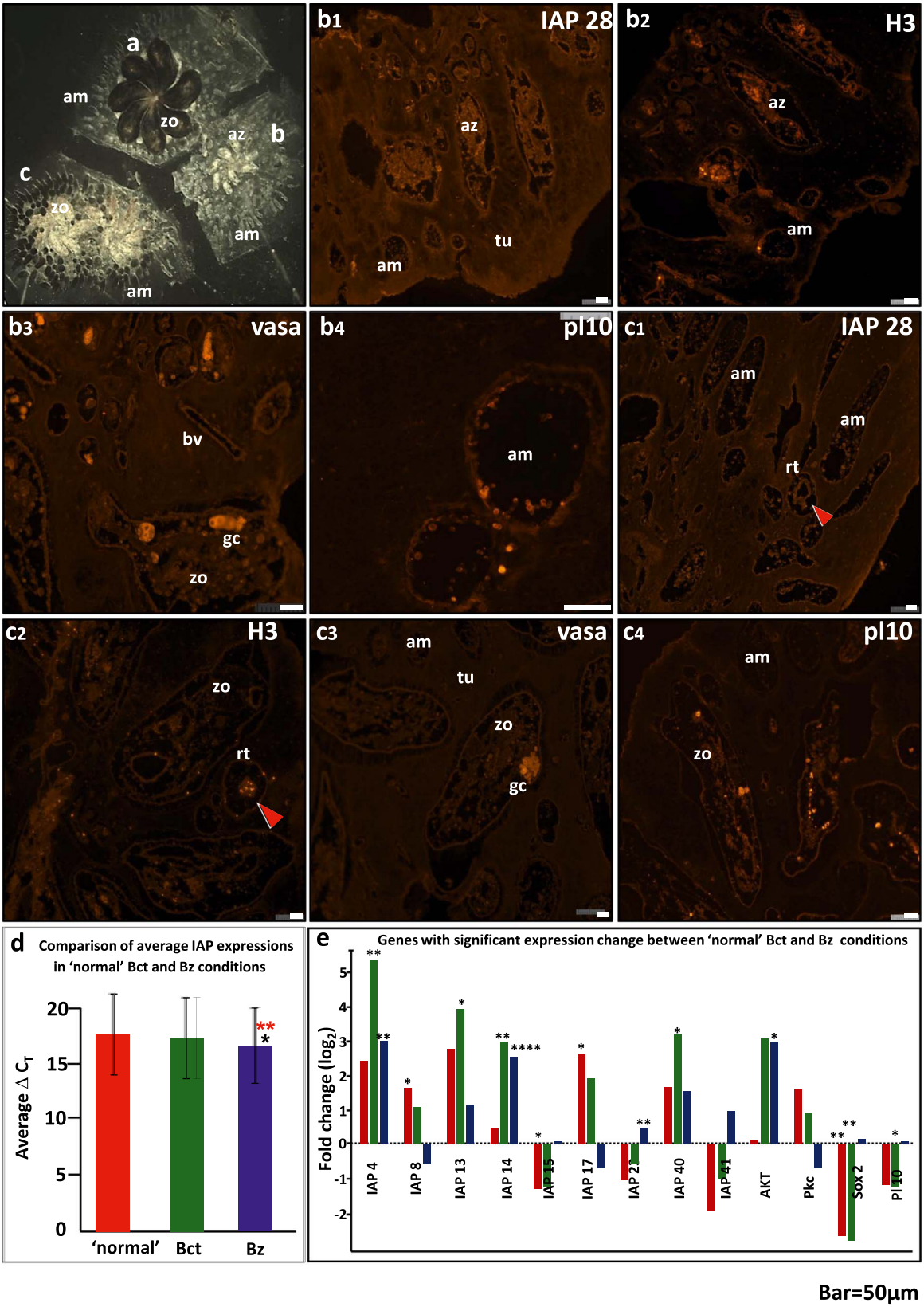

Fig. 7. Budectomy in isolated colony as compared to budectomy in system connected via a single blood vessel to an intact system. A colony divided into three ramets, each subjected to a different treatment: (a) intact ramet (b) a ramet that was completely budectomized and connected via one blood vessel to an the intact ramet (Bct ramets); (c) ramet c, isolated from the other two ramets, was also budectomized (Bz ramets). Immunological analyses were performed on sections form those budectomized tissue. Sections b1-b4 originated from ramet b. Sections c1-c4, originated from ramet c. The sections were stained with the specific antibodies as specified on each picture. Abbreviations: am-ampulla; az-absorbed zooid; bv-blood vessel; gc-germ cells; rt-regenerating tissue; tu-tunic; zo-zooid. Red arrowheads point to regenerating tissues. Scale bar = 50 µm. (d, e) qPCR analyses of expression difference between Bz, Bct and 'normal' ramets ('normal'-ramets are whole colonies budectomized at blastogenetic stage A just before being sacrificed and processed); (d) Display the global IAP expression difference between the three conditions by comparing average ΔC_T of all IAPs calculated for each condition. Average IAP expressions are increased in Bz colonies relative to control and Bct colonies. Significant difference of Bz from 'normal' colonies: * $p < 0.05$; Significant difference of Bz from Bct colonies: ** $p < 0.005$. (e) Display expressions of genes that were significantly changed as follows: red bars represent Bct ramets' expression relative to control ramets, green bars represent Bz ramets expression relative to control ramets and blue bars represent Bz ramtes expression relative to Bct ramets. p-values: *$p < 0.05$; ** $p < 0.005$; **** -$p < 0.00005$.

Table 3
Hemi-budectomy impacts on *B. schlosseri* colonies.

Day / Genet	0	1	2	3	4	5	6	7	10	11	14	17
P1	C	C	D	A	A	A	C	C	A	B	C	A
P2	A	B	C	C	C	D	A	A	C	C	A	C
P3	C	A**	A	A	C	C	A	A	B	C	A	C
P4	A	C	C	C	D	A	B	B	C	A	C	D
P5	B	C	C	D	A	B	B	C	A	A	D	C
P6	B	C	C	C	A	A	B	C	A	A	C	A
P7	C	C	D	A	B	C	C	C	A	A	C	A
P8	A	A	B	C	D	A	A	B	B	B	C**	A
P9	C	C	A	A	B	C	C	A	B	C	A	C
P10	B	B	C	C	C	A	A	A	C	A	C	D

A, B, C, D represent different blastogenetic stages of control colonies. ** Detachment of blood connection between the budcetomized and intact systems in the colony.

- Normal phenotype
- Giant ampullae loaded with blood cells
- Chaos stage-tightly packed zooids and ampullae
- Appearance of regeneration centers
- Formation of zooids
- Formation of a first 'system'
- Partially absorbed zooids
- Completely absorbed zooids
- Partially absorbed blood vessel
- Clearance of remains of old zooid and return to normal phenotype

Daily phenotype follow-up on hemi-budectomized colonies in which one blood vessel connected between a budectonized system and an intact system (Bct) in each colony. Ten colonies were observed throughout the 17 days following hemi-budectomy (day=0). The observed outcomes are marked by different colors, denoted in the table along with the blastogenetic stages of the genetically matched controls (labelled as A-D).

3.9. Impacts of the Wnt agonist

Wnt agonist (WA) is a small molecule that activates the Wnt/β-catenin pathway and causes up-regulation of target genes that drive mitosis. Administration of WA reduces inflammatory response and apoptosis (Kuncewitch et al., 2013). The Wnt/β-catenin signaling pathway also regulates the expression of some of the IAP genes like survivin (Zhu et al., 2010) and livin (Yuan et al., 2007). The impacts of administering the WA to *B. schlosseri* colonies (Rosner et al., 2014) were categorized into three major changes. These include: (1) a delayed takeover process, via a drop in nuclear β-catenin expression in the zooid's endostyle zone 4, and premature destruction of the zooid's internal organs on blastogenesis day four, accompanied by migration of phagocytes out of the cell islands; (2) arrested primary bud differentiation; and (3) minor changes in colony pattern formation. To find the impacts of WA on IAP expressions, 12 colonies at blastogenetic stage A or B were treated for 24 h with WA (agonist's incubation day has been assigned as day 1; Fig. 9a,b) and closely monitored for up to 22 days. Colonies retained their normal phenotype until they cycled into blastogenetic stage D (Fig. 9b, c). We recorded a prolonged takeover

Table 4
Budectomized colonies treated with GDC-0152.

Day / Genet	0	1	2	3	4	5	6	7	8	9	10		13	14	16	17	20	23	27	31
B1	C	C	C	D	A	A	B	C	C	C	D		B	C	C	C	A	C	A	C
B7	D	A	A	B	B	C	C	C	A	A										
B9	C	C	D	A	B	B	C	C	C	C	D		B	C	C	C	A	C	A	C
B17	D	A	A	B	B	C	D	A	A	B										
B19	C	A	D	A	B	B	C	C	C	D										
B1bis										C										
B7bis										A										
B9bis										C										
B17bis										B										
B19bis										D										

Water refresh

A, B, C, D represent different blastogenetic stages of the control.

- Normal phenotype
- Giant ampullae loaded with blood cells
- Chaos stage, tightly packed zooids and ampullae
- Appearance of regeneration centers
- Formation of zooids
- Zooids with open syphons
- Formation of a first 'system'
- Clearance of remains of old zooid and return to normal phenotype
- Death of the colony

Daily follow-up on whole body regeneration of budectomized colonies (Bz) that were subjected to 1mg/liter of GDC-0152 dissolved in seawater. Each of the five colonies was separated into two ramets by cutting a piece of tissue between two systems. One pair of each genet was budectomized, then the slides were submerged in tanks containing GDC-0152 (day=0). The other pair was budectomized 9 days later and assigned the same name as its matched pair with the suffix 'bis'. The observed outcomes are marked by different colors, denoted in the table along with the blastogenetic stages of the genetically matched controls (labelled as A-D).

phase, lasting 2–3 days instead of 24–36 h (Fig. 9d-f), where buds replaced existing zooids (Fig. 9g), revealing similar phenotypes to colonial systems at takeover, and immediately thereafter, to that of budectomized colonies (Fig. 9f,g), with tightly packed zooids, partially covered by black ampullae. After several additional blastogenetic cycles, about 25% of the colonies survived and returned to their normal phenotype.

Average ΔC_T of all IAP gene expressions during the first takeover process (blastogenetic stage D) following WA administration, were significantly higher than the ΔC_T average values in their matched controls at blastogenetic stage D (Fig. 9h), suggesting a decrease in IAP gene expressions following WA treatment. We further analyzed other genes known to be targets of the Wnt pathway (Myc, Sox2, β-Catenin, Brachyury, Cdc25 and Snai1), and again, their average expressions were down regulated following WA treatment (Fig. 9h). Fig. 9i illustrates IAP genes that were significantly affected by the WA treatment. Most of the IAP genes were down regulated following the treatment, besides IAP10 that was as well upregulated during budectomy-induced regeneration (Fig. 7al). IAP8 was down regulated relative to normal stage D and upregulated relative to stage A as in normal colonies. Sox2 and Myc, two of the genes that are normally targeted by Wnt pathway activation, were down-regulated as compared to controls. The other two genes that were down-regulated during the WA treatment belong to the HSP90 group of proteins. Altogether, these results suggest that administration of WA to *B. schlosseri* resulted in down-regulation of most of the IAP genes, of Wnt pathway target genes, and of genes participating in the activation of the Wnt pathway.

Immunohistochemistry of WA treated colonies at blastogenetic

Table 5
Budectomized colonies treated with Birinapant.

Day / Genet	0	1	2	3	4	5	6	7	8	9	10	Water refresh	13	14	16	17	20	23	27	31
B3	B	B	C	C	C	A	D	A	B	C	A		C	C	D	A				
B5	A	A	A	B	C	D	A	C	C	C										
B8	C	C	D	A	B	C	C	C	C	C										
B11	B	C	C	C	A	A	B	B	C	C										
B16	D	A	A	B	B	C	C	C	D	A	A		C	C	A	A				
B3bis										C										
B5bis										C										
B8bis										C										
B11bis										C										
B16bis										A										

A, B, C, D represent different blastogenetic stages of the control.

- Normal phenotype
- Giant ampullae loaded with blood cells
- Chaos stage, tightly packed zooids and ampullae
- Appearance of regeneration centers
- Formation of zooids
- Zooids with open syphons
- Formation of a first 'system'
- Clearance of remains of old zooid and return to normal phenotype
- Death of the colony

Daily follow-up on whole body regeneration of budectomized colonies (Bz) that were subjected to 1.1 mg/liter of Birinapant dissolved in seawater. Each of the five colonies was separated into two ramets by cutting a piece of tissue between two systems. One pair of each genet was budectomized then the slides were submerged in tanks containing Birinapant (day=0). The other pair was budectomized 9 days later and assigned the same name as its matched pair with the suffix 'bis'. The observed outcomes are marked by different colors, denoted in the table along with the blastogenetic stages of the genetically matched controls (labelled as A-D).

stage D was performed using anti-IAP28 (Fig. 9j-o) and anti-Pl10 antibodies (Fig. 9q-u). Internal organs' impairment was observed in all zooids and in the majority of the primary buds (Fig. 9j). IAP28$^+$ phagocytes were sporadically dispersed between the deteriorating organs in zooids and buds, but not in the intact primary buds (Fig. 9k). We also documented large numbers of IAP28$^+$ phagocytes infiltrating the blood vessels and aggregating in the tunic, in close proximity to the blood vessels (Fig. 9l, o). In the WA treated zooids (Fig. 9m), as in normal blastogenetic stage D zooids (Fig. 3i), additional IAP28$^+$ cell types (unidentified) were spotted, either attached to the endostyle and the atrial epithelium or dispersed in the zooid. IAP28$^+$ ampullar pad cells were observed in some ampullae (Fig. 9n). While PL10 antibodies stains heavily soma tissues and early differentiating germ cells in regular buds (Rosner et al., 2006; Fig. 9p) in WA treated colonies the failing internal organs are only partially stained (Fig. 9q, r). Pl10 antibodies stained phagocytes at the same locations as IAP28 antibodies (Fig. 9q-s), suggesting that most of the IAP28$^+$PL10$^+$ phagocytes infiltrated the blood vessels and invaded the tunic. A fraction of this cell population was observed in the zooids and fading buds. In addition, Pl10 antibodies stained another blood cell population located in the ampullae and blood vessels (Fig. 9t,u).

4. Discussion

The IAP gene family has so far drawn very little attention in studies on tunicates, primarily in those that searched for apoptosis in developmental biology processes like embryogenesis, metamorphosis and astogeny. The few existing examples include a study on IAP gene expressions during larval metamorphosis in the solitary ascidian *Boltenia villosa* (Davidson et al., 2003), and two papers (Campagna et al., 2016; Franchi et al., 2016) on the expression patterns of two IAP genes in *B. schlosseri*. Franchi et al. (2016) revealed the expression of a single IAP gene (accession number KU948203.1; IAP10 in this study) in spreading phagocytes and undifferentiated blood cells. Campagna et al. (2016)

Table 6
Budectomized colonies treated with DMSO.

Day / Genet		0	1	2	3	4	5	6	7	9	10	12	13		16	19	23	27
c1	DMSO	A	B	C	C	C	D	A	A	B	C	C	C	Water refresh	A			
c2		C	D	A	A	B	B	C	C	D/A	A	A	B		C			
c3		A	B	C	C	A	B	B	C	D	A	A	B		D	C	A	C
c4		C	D	A	A	B	B	C	C	A	A	C	D		A	C	C	B
c5		B	C	D	A	A	B	B	C	D	A	B	A		B	C	B	B

A, B, C, D represent different blastogenetic stages of the control.

Normal phenotype

Giant ampullae loaded with blood cells

Chaos stage, tightly packed zooids and ampullae

Appearance of regeneration centers

Formation of zooids

Clearance of remains of old zooid and return to normal phenotype

Death of the colony

Daily follow-up on the whole body regeneration process following complete budectomy of five colonies (Bz) and incubation in seawater containing 100µl DMSO/liter seawater (day=0). The observed outcomes are marked by different colors, denoted in the table along with the blastogenetic stages of the genetically matched controls (labelled as A-D).

detailed the mRNA upregulation of another IAP gene (IAP8 in this study) before and during the takeover phase of blastogenesis. Here, for the first time, we focused on the IAP family of genes in *B. schlosseri* with an emphasis on two developmental biology processes, the typical botryllid ascidians astogeny (blastogenesis), and a budectomy-induced whole body regeneration in this species.

Results show that the *B. schlosseri*'s genome includes 25 IAP genes that, based on their domains, belong to between 9 and 11 subfamilies. This list of IAP genes is a considerably more detailed than the one found in *Ciona intestinalis* (12 IAP genes; UniProtKB protein database). The BIR domain (characteristic to IAP genes) enables the IAP molecule to interact with casapases, IAP inhibitors, and TRAF1/2. The second common domain found in the IAP genes is the RING (in 16 *B. schlosseri*'s IAP genes), endowing ubiquitination of various molecules (including of other IAPs genes), the early step for protein destruction or functionality modifications (Blankenship et al., 2009; Gyrd-Hansen and Meier, 2010; Hao et al., 2004; Lopergolo et al., 2009; Qiu and Goldberg, 2005).

Regulation of IAPs is known to be exerted at both the transcriptional (Chen et al., 2016; Crippa et al., 2016; Zhu et al., 2010) and posttranslational levels (Fuchs et al., 2013; Garcia-Fernandez et al., 2010; Nogueira-Ferreira et al., 2013; Wei et al., 2008), two approaches that we used here to study and characterize IAP genes in *B. schlosseri*. Thus, this study involved whole colonial assays, qPCR and histochemical analyses, IAP genes blocking, studying the expression of pro-apoptotic proteins (AIF1, Bax, MCl1) and caspases (caspase 2, caspase 9, caspase 3 and two orthologues of caspase 7), the application of an apoptosis inducing agent, treatment with a WA, zooidectomy and studying the co-expression of other relevant genes including Pl10, Vasa and pH3. We also studied protein IAP28's expression patterns in various colonial tissues and by employing biological manipulations.

Our main results reveal that ten of the IAP's mRNAs were significantly upregulated at blastogenetic stages C and D, concurrent with increased expressions of apoptosis inducing genes (AIF1, Bax, MCl1) and three caspases (caspase 2 and two orthologues of caspase 7). Many of these takeover associated IAPs were also upregulated at blastogenetic stage A in response to apoptosis and necroptosis inducing treatments (100 µM H_2O and 1000 µM H_2O_2, respectively). Blastogenetic stage D, the 'takeover stage', culminates in apoptosis and zooid absorption (Lauzon et al., 1993), but goes also through processes of bud and germ cell differentiation, massive traffic of bloods cells, and reorganization of the colonial architecture (Rinkevich et al.,

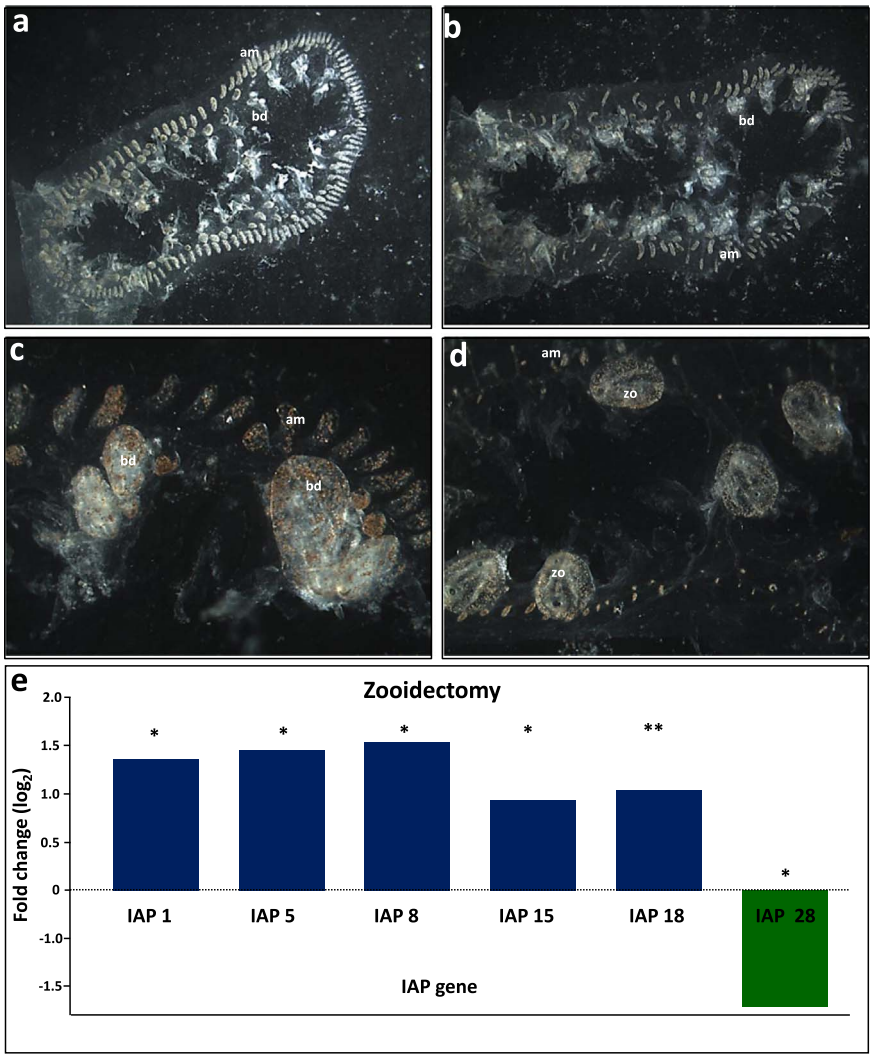

Fig. 8. Impacts of zooidectomy on *B. schlosseri* colonies. (a-d) the phenotypes of a colony following zooidectomy. (a) Immediately after the surgical procedure; (b) Two days following zooidectomy; (c) One day before opening of the siphons; (d) After opening of the siphons and the transformation of buds into zooids. Abbreviations: am-ampulla; bd-bud; zo-zooid; (e) Relative qPCR quantification of genes expressions in zooidectomized *B. schlosseri* colonies statistically examined by paired *t*-test. The analysis compares zooidectomized tissue to their matched stage D controls. IAP genes that were significantly altered are presented. p –values: *- p value < 0.05; **- p value < 0.005.

2013; Rosner et al., 2006, 2013), all developmental routes that the takeover associated IAPs' might take part in. Indeed, further examination of IAP in the different colonial modules revealed that IAP9 and IAP21 were associated with bud differentiation, while IAP8 that was already shown to be linked with these stages (Campagna et al., 2016) and IAP28 were upregulated in blastogenesis stage D zooids. Both IAP8 and IAP28 have a similar structure of two BIR domains at the N-terminal end of the molecule and a RING domain at the C-terminus. However, they are clearly distinct from each other, in being only 39% identical at the protein level, with no significant similarity at the nucleic acid level.

We further attempted to clarify the complexity of blastogenesis by utilizing two major morphological manipulations: zooidectomy and budectomy. Zooidectomy in blastogenetic stage A colonies did not affect the route of blastogenesis and was followed by normal development of the primary and secondary buds, while delaying the takeover phase by only a few hours. mRNAs of IAP8 and IAP18, two genes with highlighted expression in the takeover process, were further significantly upregulated, while IAP 28 was downregulated, in zooidectomized colonies (before the opening of the siphons), compared to their matched blastogenetic stage D controls. These results demonstrate that the two genes (IAP8 and IAP28) have different functions, while showing comparable expression patterns along blastogenesis.

As in zooidectomy, a complete budectomy did not affect the progression of the existing blastogenetic cycle, nor the colonial architecture, where the zooids in the budectomized colony did not differ from naive controls. However, the takeover phase (blastogenetic stage D; started at the same time as the controls) was characterized by the unique enhanced expression of IAP1, IAP10, IAP13, further increase in IAP14 and the upregulation of the apoptosis inhibiting PI3K-Akt Pathway (Akt and Pik3cA) that we considered as associated with budectomy. The PI3K/Akt pathway activation is known to be associated with pro-survival pathways, and Akt has been previously shown to be regulated by a XIAP, a human IAP protein (Gagnon et al., 2008). As expected, low expressions of Sox2 and Myc, bud associated genes, were detected. Following budectomy the colony might undergo a whole body regeneration (WBR), or absorption, depending on the existence of a functional bud. In contrast to a regular blastogenesis process, a WBR process in budectomized colonies started from the remains of the absorbed zooids and ampullae, culminating in func-

tional zooids, rising like a phoenix from the ashes. The IAP genes that were associated with this process included IAP4 and IAP14. Whenever there was a blood vessel connection between the budectomized system and functional buds (Bct colonies), the WBR was not initiated, and the zooids were absorbed. The absorption of the whole cohort of functional zooids was considerably slower nonetheless, and their heartbeats were still detected days after they ceased in the controls. Even after complete destruction of the internal organs in the budectomized part of the Bct assay, some cells remained alive and were able to divide. Among these left behind cells there were many small (5 μm) Pl10^{+} cells with

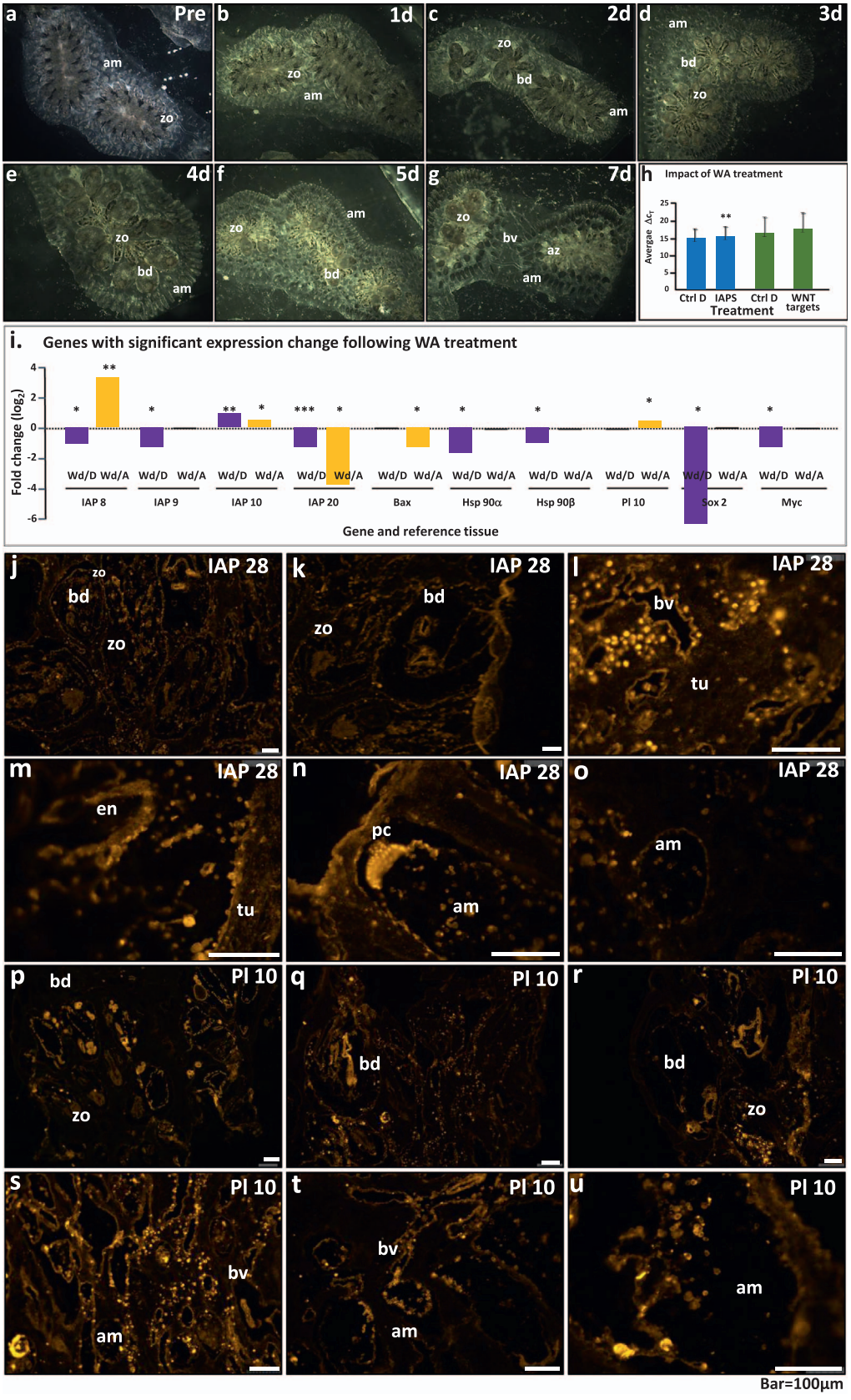

Fig. 9. Impact of Wnt agonist on *B. schlosseri* blastogenetic cycle. (a-g) Follow-up after colony treated with WA. (a) the colony pre incubation; (b) the colony after 24 h of incubation with WA; (c) the colony after transfer to clean seawater; (d-f) The colony has been undergoing a three day long takeover phase; (g) several primary buds in the colony enter blastogenetic stage A and start a new blastogenetic cycle; (h, i) Expressions of IAP genes and some Wnt/β-cat pathway target genes following WA treatment tested by qPCR and paired *t*-test analyses. (h) Comparison of average ΔC_T of genes in stage D WA treated colonies to stage and genet matched controls. The compared groups are; (blue bars) all tested IAP genes, (green bars) Wnt target genes. Significant decrease in IAP gene expression are detected in WA treated colonies. (i) The chart only illustrates genes that are significantly altered. Purple bars represent a comparison of stage D treated colony versus their genetic matched normal stage D controls. Yellow bars represent a comparison of stage D treated colony versus their genetic matched normal stage A controls. Abbreviations: Wd-WA agonist treated colony at stage D; Wd/D-relative expression of Wd colonies versus their naïve matched controls at stage D. Wd/A-relative expression of Wd colonies versus their naïve matched controls at stage A. p-values: * < 0.05; ** < 0.005; *** < 0.0005. (j-o,q-u)-Immunohistochemical analyses of WA treated colonies at blastogenetic stage D. (p) Naive normal colony; The Sections were stained with (j-o) polyclonal anti-IAP28 antibodies and (p-u) polyclonal anti-Pl10 antibodies. Abbreviations: am-ampulla; az-absorbed zooid; bv-blood vessel; bd-primary bud; en-endostyle; pc-pad cells; tu-tunic; z-zooid; Bar = 100 μm.

relatively large nuclei that resemble stem cells. Expressions of IAP8 and IAP17 were upregulated in these tissues and that might correlate to the survival of these left behind cells.

We also revealed a simultaneous expression of apoptosis inhibitors and apoptosis inducers in normal blastogenetic stage D zooids, where massive apoptosis and phagocytosis took place (Lauzon et al., 1993). This contradiction can be explained by results demonstrating that many blood cells besides phagocytes are kept functional, thus transmitted to the next generations of zooids during takeover. These include stem cells of the germ lineage (Rosner et al., 2013) and soma stem cell (Rinkevich et al., 2013; Voskoboynik et al., 2008) lineages that dwell in temporal niches (cell islands, endostyle, branchial sac and digestive system) and during takeover, they migrate to the developing zooids. This might also highlight the connections between two major development/regeneration processes in *B. schlosseri,* the vascular budding (Sabbadin et al., 1975; Voskoboynik et al., 2007) and WBR following budectomy (described here for the first time) at the takeover phase of blastogenesis. We further elucidate here common IAP upregulation in takeover and WBR (IAP8, IAP14, IAP16, IAP28, IAP41) that have dual expressions in apoptosis and regeneration. This reminiscences what is called “apoptosis-induced compensatory proliferation” (Bergmann and Steller, 2010; Fan and Bergmann, 2008) phenomenon, demonstrated in several model animals like *Drosophila*, *Hydra*, planarians, *Xenopus*, newt and mouse. Further, Yosefzon et al. (2018) showed that casapse3 activates YAP that promotes cell proliferation in a process that is also associated with upregulated XIAP, a human IAP orthologue mRNA.

We chose IAP28 for detailed work since this gene is associated with the absorbed zooids at the takeover phase. Staining of *B. schlosseri* tissues with IAP28-specific antibodies at various blastogenetic stages, revealed that in addition to its highlighted expression in blastogenetic stage D zooids, IAP^+ cells were blood cells, germ cells, central ganglions (in zooids and buds), cells in the zooidal stomach, embryonic cells and test cells that wrap oocytes and embryos. Moreover, the high IAP28 protein expression in blastogenetic stage D is probably due to phagocytes, heavily stained by IAP28 mainly at stage D and in 100 μM H_2O_2 treated tissue (where phagocytes are activated). This enhanced phagocytic activity during the *B. schlosseri* takeover phase was suggested as a regulating mechanism for the massive wave of apoptosis (Voskoboynik et al., 2004), in a similar way to phagocytosis induced apoptosis in mammals (Kennedy and DeLeo, 2009) and in invertebrates (Coates et al., 2013). Throughout the takeover process, recruited phagocytes ingest the dying cells and thereafter undergo a phagocytosis-induced-apoptosis process, culminating in their engulfment by other phagocytes (Franchi et al., 2016). This phagocytosis-induced apoptosis has been studied further in our experimental manipulations. In early blastogenetic stage D budectomized colonies, phagocytosis is practically stopped and IAP+Pl10+ expression is declined and is resumed later, in concert with the appearance of $IAP28^+Pl10^+$ phagocytes that remove the remains of the old generation of zooids. Infiltration of many $IAP28^+Pl10^+$ phagocytes into the tunic was recorded during takeover arrest (lasting 2–3 days instead of 24–36 h), following the administration of a WA. WA induced takeover arrest was also associated with global reduction of IAP genes expressions, except of IAP8 and IAP10 that were upregulated.

IAP28 protein was also abundant in the nuclei of test cells of the egg's outer layer and in the tunic wrapping the embryos. Such nuclear localization recorded with two IAP proteins (human cIAP1 and survivin) had been correlated with cell proliferation control (Samuel et al., 2005) and their translocation to the cytoplasm has been associated with apoptosis signals that activate caspases. Nuclear expression of IAPs was also associated with several types of cancers with poor prognosis (Dubrez et al., 2013). In *Ciona intestinalis,* test cells at the periphery of embryos undergo spatial and temporal apoptosis, initiated by the activation of the NF-κB pathway (Maury et al., 2006), where test cells closer to the embryonic tissue survived longer than those in the periphery. In corroboration, we (Rosner et al., 2006) documented expressions of Pl10, another modulator of the NF-κB pathway, in the test cells. We thus suggest that test cell longevity is mediated through IAP28, Pl10 dependent NF-κB activation.

Inhibition of IAP functions by GDC-0152 caused specific malformation in most studied colonies, including damages to buds, zooids, blood vessels and ampullae, and the desynchronization of the takeover process. Treating colonies with GDC-0152 before budectomy for a prolonged period, resulted in failure of budectomy induced WBR. Administration of GDC-0152 caused increased expressions of caspase 9 (an initiator caspase of the intrinsic pathway) as previously reported (Hu et al., 2015), and an increase in IAP and Akt mRNA at blastogenetic stage A, in contrast to mammalian cells where a decrease in IAP and Akt proteins was described in leukemia cells (Hu et al., 2015). It is especially intriguing that GDC-0152 administration caused upregulation of many IAPs at blastogenetic stage A, but not of IAP genes associated with takeover (IAP8, IAP16, IAP21 and IAP28). Similar upregulation of IAP gene mRNA did not occur during blastogenetic stage D (with the exception of IAP21). The explanation for these mismatching findings could be that the increase in mRNA is a compensatory mechanism to the reduction in the quantity of the protein of the appropriate gene. Additional correlations between IAP and the Akt pathway were also demonstrated in this research in budectomy induced WBR.

Understanding the molecular mechanisms behind the tight control of IAP gene expressions that has been demonstrated here, and the biological phenomena of astogeny and regeneration in botryllid ascidians, might help to elucidate evolutionary roots and common functions for the IAP gene families.

Acknowledgements

We thank N. Cohen and M. Kaufman for technical assistance, M. Michael for language editing and G. Paz for artistic work. This research was supported by the Israel Science Foundation (no. 172/17) and by the United States – Israel Binational Science Foundation (no. 2015012).

Appendix A. Supporting information

Supplementary data associated with this article can be found in the online version at doi:10.1016/j.ydbio.2018.10.015.

References

Altieri, D.C., 2015. Survivin – the inconvenient IAP. Semin. Cell Dev. Biol. 39, 91–96. http://dx.doi.org/10.1016/j.semcdb.2014.12.007.

Ballarin, L., Schiavon, F., Manni, L., 2010. Natural apoptosis during the blastogenetic cycle of the colonial ascidian *Botryllus schlosseri*: a morphological analysis. Zool. Sci. 27, 96–102. http://dx.doi.org/10.2108/zsj.27.96.

Ballarin, L., Burighel, P., Cima, F., 2008. A tale of death and life: natural apoptosis in the colonial ascidian *Botryllus schlosseri* (Urochordata, Ascidiacea). Curr. Pharm. Des. 14, 138–147.

Berrill, N.J., 1950. The Tunicata with an Account of the British Species. Ray Society, London.

Berrill, N.J., 1951. Regeneration and budding in tunicates. Biol. Rev. 26, 456–475.

Blankenship, J.W., Varfolomeev, E., Goncharov, T., Fedorova, A.V., Kirkpatrick, D.S., Izrael-Tomasevic, A., Phu, L., Arnott, D., Aghajan, M., Zobel, K., Bazan, J.F., Fairbrother, W.J., Deshayes, K., Vucic, D., 2009. Ubiquitin binding modulates IAP antagonist-stimulated proteasomal degradation of c-IAP1 and c-IAP2(1). Biochem. J. 417, 149–160. http://dx.doi.org/10.1042/BJ20081885.

Bergmann, A., Steller, H., 2010. Apoptosis, stem cells, and tissue regeneration. Sci. Signal. 3, re8. http://dx.doi.org/10.1126/scisignal.3145re8.

Budhidarmo, R., Day, C.L., 2015. IAPs: modular regulators of cell signaling. Semin. Cell Dev. Biol. 39, 80–90. http://dx.doi.org/10.1016/j.semcdb.2014.12.002.

Campagna, D., Gasparini, F., Franchi, N., Vitulo, N., Ballin, F., Manni, L., Valle, G., Ballarin, L., 2016. Transcriptome dynamics in the asexual cycle of the chordate *Botryllus schlosseri*. BMC Genom. 17, 275. http://dx.doi.org/10.1186/s12864-016-2598-1.

Chen, X., Duan, N., Zhang, C., Zhang, W., 2016. Survivin and tumorigenesis: molecular mechanisms and therapeutic strategies. J. Cancer 7, 314–323. http://dx.doi.org/10.7150/jca.13332.

Cima, F., Manni, L., Basso, G., Fortunato, E., Accordi, B., Schiavon, F., Ballarin, L., 2010. Hovering between death and life: natural apoptosis and phagocytes in the blastogenetic cycle of the colonial ascidian *Botryllus schlosseri*. Dev. Comp. Immunol. 34, 272–285. http://dx.doi.org/10.1016/j.dci.2009.10.005.

Coates, C.J., Whalley, T., Wyman, M., Nairn, J., 2013. A putative link between phagocytosis-induced apoptosis and hemocyanin-derived phenoloxidase activation. Apoptosis 18, 1319–1331. http://dx.doi.org/10.1007/s10495-013-0891-x.

Crippa, E., Folini, M., Pennati, M., Zaffaroni, N., Pierotti, M.A., Gariboldi, M., 2016. miR-342 overexpression results in a synthetic lethal phenotype in BRCA1-mutant HCC1937 breast cancer cells. Oncotarget 7, 18594–18604.

Dallaglio, K., Marconi, A., Pincelli, C., 2012. Survivin: a dual player in healthy and diseased skin. J. Infect. Dis. 132, 18–27. http://dx.doi.org/10.1038/jid.2011.279.

Davidson, B., Smith Wallace, S.E., Howsmon, R.A., Swalla, B.J., 2003. A morphological and genetic characterization of metamorphosis in the ascidian *Boltenia villosa*. Dev. Genes. Evol. 213, 601–611. http://dx.doi.org/10.1242/jeb.01045.

De Maria, A., Bassnett, S., 2015. Birc7: a late fiber gene of the crystalline lens. Investig. Ophthalmol. Vis. Sci. 56, 4823–4834.

De Tomaso, T., (UCSB), Tiozzo, S., (Biodev, OOV), Gracey, A. (USC), Philippe, D. (Biodev, OOV) and this site (Tony De Tomaso (UCSB), Stefano Tiozzo (Biodev, OOV), Gracey, A. (USC), Philippe Dru P. (Biodev, OOV), 2012. ⟨http://octopus.obsvlfr.fr/public/botryllus/blast_botryllus.php⟩.

Dubrez, L., Berthelet, J., Glorian, V., 2013. IAP proteins as targets for drug development in oncology. OncoTargets Ther. 9, 1285–1304. http://dx.doi.org/10.2147/OTT.S33375.

Estornes, Y., Bertrand, M.J., 2015. IAPs, regulators of innate immunity and inflammation. Semin Cell. Dev. Biol. 39, 106–114. http://dx.doi.org/10.1016/j.semcdb.2014.03.035.

Fan, Y., Bergmann, A., 2008. Apoptosis-induced compensatory proliferation. The Cell is dead. Long live the Cell!. Trends Cell Biol. 18, 467–473. http://dx.doi.org/10.1016/j.tcb.2008.08.001.

Finlay, D., Teriete, P., Vamos, M., Cosford, N.D.P., Vuori, K., 2017. Inducing death in tumor cells: roles of the inhibitor of apoptosis proteins. F1000Research 6, 587.

Franchi, N., Ballin, F., Manni, L., Schiavon, F., Basso, G., Ballarin, L., 2016. Recurrent phagocytosis-induced apoptosis in the cyclical generation change of the compound ascidian *Botryllus schlosseri*. Dev. Comp. Immunol. 62, 8–16. http://dx.doi.org/10.1016/j.dci.2016.04.011.

Fuchs, Y., Brown, S., Gorenc, T., Rodriguez, J., Fuchs, E., Steller, H., 2013. Sept4/ARTS regulates stem cell apoptosis and skin regeneration. Science 341, 286–289.

Fulda, S., 2014a. Inhibitor of Apoptosis (IAP) proteins in hematological malignancies: molecular mechanisms and therapeutic opportunities. Leukemia 28, 1414–1422. http://dx.doi.org/10.1038/leu.2014.56.

Fulda, S., 2014b. Regulation of cell migration, invasion and metastasis by IAP proteins and their antagonists. Oncogene 33, 671–676. http://dx.doi.org/10.1038/onc.2013.63.

Gagnon, V., Van Themsche, C., Turner, S., Leblanc, V., Asselin, E., 2008. Akt and XIAP regulate the sensitivity of human uterine cancer cells to cisplatin, doxorubicin and taxol. Apoptosis 13, 259–271.

Garcia-Fernandez, M., Kissel, H., Brown, S., Gorenc, T., Schile, A.J., Rafii, S., Larisch, S., Steller, H., 2010. Sept4/ARTS is required for stem cell apoptosis and tumor suppression. Genes Dev. 24, 2282–2293.

Gyrd-Hansen, M., Meier, P., 2010. Nat. Rev. Cancer 10, 561–574. http://dx.doi.org/10.1038/nrc2979.

Hao, Y., Sekine, K., Kawabata, A., Nakamura, H., Ishioka, T., Ohata, H., Katayama, R., Hashimoto, C., Zhang, X., Noda, T., Tsuruo, T., Naito, M., 2004. Apollon ubiquitinates SMAC and caspase-9, and has an essential cytoprotection function. Nat. Cell Biol. 6, 849–860.

Hu, R., Li, J., Liu, Z., Miao, M., Yao, K., 2015. GDC-0152 induces apoptosis through down-regulation of IAPs in human leukemia cells and inhibition of PI3K/Akt signaling pathway. Tumor Biol. 36, 577–584. http://dx.doi.org/10.1007/s13277-014-2648-8.

Kawamura, K., Tachibana, M., Sunanaga, T., 2008. Cell proliferation dynamics of somatic and germline tissues during zooidal life span in the colonial tunicate *Botryllus primigenus*. Dev. Dyn. 237, 1812–1825. http://dx.doi.org/10.1002/dvdy.21592.

Kennedy, A.D., DeLeo, F.R., 2009. Neutrophil apoptosis and the resolution of infection. Immunol. Res. 43, 25–61. http://dx.doi.org/10.1007/s12026-008-8049-6.

Krepler, C., Chunduru, S.K., Halloran, M.B., He, X., Xiao, M., Vultur, A., Villanueva, J., Mitsuuchi, Y., Neiman, E.M., Benetatos, C., Nathanson, K.L., Amaravadi, R.K., Pehamberger, H., McKinlay, M., Herlyn, M., 2013. The novel SMAC mimetic birinapant exhibits potent activity against human melanoma cells. Clin. Cancer Res. 19, 1784–1794. http://dx.doi.org/10.1158/1078-0432.CCR-12-2518.

Kuncewitch, M., Yang, W.L., Molmenti, E., Nicastro, J., Coppa, G.F., Wang, P., 2013. Wnt agonist attenuates liver injury and improves survival after hepatic ischemia/reperfusion. Shock 39, 3–10. http://dx.doi.org/10.1097/SHK.0b013e3182764fe8.

Lauzon, R.J., Patton, C.W., Weissman, I.L., 1993. A morphological and immunohistochemical study of programmed cell death in *Botryllus schlosseri* (Tunicata, Ascidiacea). Cell Tissue Res. 272, 115–127. http://dx.doi.org/10.1007/BF00323577.

Lauzon, R.J., Ishizuka, K.J., Weissman, I.L., 2002. Cyclical generation and degeneration of organs in a colonial urochordate involves crosstalk between old and new: a model for development and regeneration. Dev. Biol. 249, 333–348.

Lopergolo, A., Pennati, M., Gandellini, P., Orlotti, N.I., Poma, P., Daidone, M.G., Folini, M., Zaffaroni, N., 2009. Apollon gene silencing induces apoptosis in breast cancer cells through p53 stabilization and caspase-3 activation. Br. J. Cancer 100, 739–746.

Ma, L., Huang, Y., Song, Z., Feng, S., Tian, X., Du, W., Qiu, X., Heese, K., Wu, M., 2006. Livin promotes Smac/DIABLO degradation by ubiquitin-proteasome pathway. Cell Death Differ. 13, 2079–2088. http://dx.doi.org/10.1038/sj.cdd.4401959.

Martin, S.J., 2004. An Apollon vista of death and destruction. Nat. Cell Biol. 6, 804–806.

Maury, B., Martinand-Mari, C., Chambon, J.P., Soulé, J., Degols, G., Sahuquet, A., Weill, M., Berthomieu, A., Fort, P., Mangeat, P., Baghdiguian, S., 2006. Fertilization regulates apoptosis of Ciona intestinalis extra-embryonic cells through thyroxine (T4)-dependent NF-kappaB pathway activation during early embryonic development. Dev. Biol. 289, 152–165. http://dx.doi.org/10.1016/j.ydbio.2005.10.021.

Manni, L., Gasparini, F., Hotta, K., Ishizuka, K.J., Ricci, L., Tiozzo, S., Voskoboynik, A., Dauga, D., 2014. Ontology for the asexual development and anatomy of the colonial chordate *Botryllus schlosseri*. PLOS One 9, e96434. http://dx.doi.org/10.1371/journal.pone.0096434.

Manni, L., Zaniolo, G., Cima, F., Burighel, P., Ballarin, L., 2007. *Botryllus schlosseri*: a model ascidian for the study of asexual reproduction. Dev. Dyn. 236, 335–352. http://dx.doi.org/10.1002/dvdy.21037.

Milkman, R., 1967. Genetic and developmental studies on *Botryllus schlosseri*. Biol. Bull. 132, 229–243.

Mukai, H., Watanabe, H., 1976a. Relation between sexual and asexual reproduction in the compound ascidian, *Botryllus* primigenus. Sci. Rep. Fac. Educ. Gumma Univ. 25, 61–79.

Mukai, H., Watanabe, H., 1976b. Studies on the formation of germ cells in compound ascidian *Botryllus* primigenus Oka. J. Morphol. 148, 337–362.

Nogueira-Ferreira, R., Vitorino, R., Ferreira-Pinto, M.J., Henriques-Coelho, T., 2013. Exploring the role of post-translational modifications on protein–protein interactions with survivin. Arch. Biochem. Biophys. 538, 64–70. http://dx.doi.org/10.1016/j.abb.2013.07.027.

O'Riordan, M.X., Bauler, L.D., Scott, F.L., Duckett, C.S., 2008. Inhibitor of apoptosis proteins in eukaryotic evolution and development: a model of thematic conservation. Dev. Cell 15, 497–508.

Perimenis, P., Galaris, A., Voulgari, A., Prassa, M., Pintzas, A., 2016. IAP antagonists Birinapant and AT-406 efficiently synergize with either TRAIL, BRAF, or BCL-2 inhibitors to sensitize BRAFV600E colorectal tumor cells to apoptosis. BMC Cancer 16, 624–639. http://dx.doi.org/10.1186/s12885-016-2606-5.

Pfaffl, M.W., 2001. A new mathematical model for relative quantification in real-time RT-PCR. Nucleic Acids Res. 29, 2002–2007.

Qiu, X.-B., Goldberg, A.L., 2005. The membrane-associated inhibitor of apoptosis protein, BRUCE/Apollon, antagonizes both the precursor and mature forms of Smac and caspase-9. J. Biol. Chem. 280, 174–182.

Rinkevich, B., 2002. The colonial urochordate *Botryllus schlosseri*: from stem cells and natural tissue transplantation to issues in evolutionary ecology. BioEssays 24, 730–740. http://dx.doi.org/10.1002/bies.10123.

Rinkevich, B., Lauzon, R.J., Brown, B.W.M., Weissman, I.L., 1992. Evidence for a programmed lifespan in a colonial protochordate. Proc. Natl. Acad. Sci. USA 89, 3456–3550.

Rinkevich, B., Shapira, M., 1998. An improved diet for inland broodstock and the establishment of an inbred line form *Botryllus schlosseri*, a colonial sea squirt (Ascidiacea). Aquat. Living Resour. 11, 163–171.

Rinkevich, Y., Paz, G., Rinkevich, B., Reshef, R., 2007. Systemic bud induction and retinoic acid signaling underlie whole body regeneration in the urochordate Botrylloides leachi. PLOS Biol. 5, e71. http://dx.doi.org/10.1371/journal.pbio.0050071.

Rinkevich, Y., Voskoboynik, A., Rosner, A., Rabinowitz, C., Paz, G., Oren, M., Douek, J., Alfassi, G., Moiseeva, E., Ishizuka, K.J., Palmeri, K.J., Weissman, I.L., Rinkevich, B., 2013. Repeated, long-term cycling of putative stem cells between niches in a basal chordate. Dev. Cell 24, 76–88. http://dx.doi.org/10.1016/j.devcel.2012.11.010.

Rosner, A., Alfassi, G., Moiseeva, E., Paz, G., Rabinowitz, C., Lapidot, Z., Douek, J., Haim, A., Rinkevich, B., 2014. The involvement of three signal transduction pathways in

botryllid ascidian astogeny, as revealed by expression patterns of representative genes. Int. J. Dev. Biol. 58, 677–692. http://dx.doi.org/10.1387/ijdb.140114ar.

Rosner, A., Moiseeva, E., Rabinowitz, C., Rinkevich, B., 2013. Germ lineage properties in the urochordate *Botryllus* schlosseri – from markers to temporal niches. Dev. Biol. 384, 356–374. http://dx.doi.org/10.1016/j.ydbio.2013.10.002.

Rosner, A., Moiseeva, E., Rinkevich, Y., Lapidot, Z., Rinkevich, B., 2009. Vasa and the germ line lineage in a colonial urochordate. Dev. Biol. 331, 113–128. http://dx.doi.org/10.1016/j.ydbio.2009.04.025.

Rosner, A., Paz, G., Rinkevich, B., 2006. Divergent roles of the DEAD-box protein BS-PL10, the urochordate homologue of human DDX3 and DDX3Y proteins, in colony astogeny and ontogeny. Dev. Dyn. 235, 1508–1521.

Rosner, A., Rabinowitz, C., Moiseeva, E., Voskoboynik, A., Rinkevich, B., 2007. BS-cadherin in the colonial urochordate *Botryllus schlosseri*: one protein, many functions. Dev. Biol. 304, 687–700. http://dx.doi.org/10.1016/j.ydbio.2007.01.018.

Sabbadin, A., Zaniolo, G., Majone, F., 1975. Determination of polarity and bilateral asymmetry in palleal and vascular buds of the ascidian *Botryllus schlosseri*. Dev. Biol. 46, 79–87. http://dx.doi.org/10.1016/0012-1606(75)90088-3.

Samuel, T., Okada, K., Hyer, M., Welsh, K., Zapata, J.M., Reed, J.C., 2005. cIAP1 localizes to the nuclear compartment and modulates the cell cycle. Cancer Res. 65, 210–218.

Schläfli, A.M., Torbett, B.E., Fey, M.F., Tschan, M.P., 2012. BIRC6 (APOLLON) is down-regulated in acute myeloid leukemia and its knockdown attenuates neutrophil differentiation. Exp. Hematol. Oncol. 1, 25. http://dx.doi.org/10.1186/2162-3619-1-25.

Silke, J., Meier, P., 2013. Inhibitor of apoptosis (IAP) proteins–modulators of cell death and inflammation. Cold Spring Harb. Perspect. Biol. 5, a008730. http://dx.doi.org/10.1101/cshperspect.a008730.

Vasilikos, L., Spilgies, L.M., Knop, J., Wei-Lynn Wong, W., 2017. Regulating the balance between necroptosis, apoptosis and inflammation by inhibitors of apoptosis proteins. Immunol. Cell Biol. 95, 160–165. http://dx.doi.org/10.1038/icb.2016.118.

Vasudevan, D., Ryoo, H.D., 2015. Regulation of cell death by IAPs and their antagonists. Curr. Top. Dev. Biol. 114, 185–208. http://dx.doi.org/10.1016/bs.ctdb.2015.07.026.

Voskoboynik, A., Neff, N.F., Sahoo, D., Newman, A.M., Pushkarev, D., Koh, W., Passarelli, B., Fan, H.C., Mantalas, G.L., Palmeri, K.J., Ishizuka, K.J., Gissi, C., Griggio, F., Ben-Shlomo, R., Corey, D.M., Penland, L., White, R.A., 3rd, Weissman, I.L., Quake, S.R., 2013. The genome sequence of the colonial chordate *Botryllus schlosseri*. Elife 2, e00569. http://dx.doi.org/10.7554/eLife.00569.

Voskoboynik, A., Simon-Blecher, N., Soen, Y., Rinkevich, B., De Tomaso, A.W., Ishizuka, K.J., Weissman, I.L., 2007. Striving for normality: whole body regeneration through a series of abnormal generations. FASEB J. 21, 1335–1344. http://dx.doi.org/10.1096/fj.06-7337com.

Voskoboynik, A., Rinkevich, B., Weiss, A., Moiseeva, E., Reznick, A.Z., 2004. Macrophage involvement for successful degeneration of apoptotic organs in the colonial urochordate *Botryllus schlosseri*. J. Exp. Biol. 207 (Pt 14), 2409–2416. http://dx.doi.org/10.1242/jeb.01045.

Voskoboynik, A., Soen, Y., Rinkevich, Y., Rosner, A., Ueno, H., Reshef, R., Ishizuka, K.J., Palmeri, K.J., Moiseeva, E., Rinkevich, B., Weissman, I.L., 2008. Identification of the endostyle as a stem cell niche in a colonial chordate. Cell Stem Cell 3, 456–464. http://dx.doi.org/10.1016/j.stem.2008.07.023.

Wei, Y., Fan, T., Yu, M., 2008. Inhibitor of apoptosis proteins and apoptosis. Acta Biochim. Biophys. Sin. 40, 278–288. http://dx.doi.org/10.1111/j.1745-7270.2008.00407.x.

Xiang, J., Wan, C., Guo, R., Guo, D., 2016. Is hydrogen peroxide a suitable apoptosis inducer for all cell types? Biomed. Res. Int. 2016, 7343965. http://dx.doi.org/10.1155/2016/7343965.

Xiang, N., He, M., Ishaq, M., Gao, Y., Song, F., Guo, L., Ma, L., Sun, G., Liu, D., Guo, D., Chen, Y., 2016. The DEAD-Box RNA helicase DDX3 interacts with NF-κB subunit p65 and suppresses p65-mediated transcription. PLOS One 11, e0164471. http://dx.doi.org/10.1371/journal.pone.0164471.

Yosefzon, Y., Soteriou, D., Feldman, A., Kostic, L., Koren, E., Brown, S., Ankawa, R., Sedov, E., Glaser, F., Fuchs, Y., 2018. Caspase-3 regulates YAP-dependent cell proliferation and organ size. Mol. Cell. 70. http://dx.doi.org/10.1016/j.molcel.2018.04.019.

Yuan, D., Liu, L., Gu, D., 2007. Transcriptional regulation of livin by beta-catenin/TCF signaling in human lung cancer cell lines. Mol. Cell Biochem. 306, 171–178.

Zhao, S., Fu, J., Liu, X., Wang, T., Zhang, J., Zhao, Y., 2012. Activation of Akt/GSK-3beta/beta-catenin signaling pathway is involved in survival of neurons after traumatic brain injury in rats. Neurol. Res. 34, 400–407. http://dx.doi.org/10.1179/1743132812Y.0000000025.

Zhu, H., Zhang, G., Wang, Y., Xu, N., He, S., Zhang, W., Chen, M., Liu, M., Quan, L., Bai, J., Xu, N., 2010. Inhibition of ErbB2 by Herceptin reduces survivin expression via the ErbB2-beta-catenin/TCF4-survivin pathway in ErbB2-overexpressed breast cancer cells. Cancer Sci. 101, 1156–1162. http://dx.doi.org/10.1111/j.1349-7006.2010.01528, (x).